CHAPTER 8

Hydrodynamics and Transport Coefficients

Chapter 7 was concerned largely with the formal definition and general properties of time-correlation functions and with the link that exists between spontaneous, time-dependent fluctuations and the response of a fluid to an external probe. The main objectives of the present chapter are, first, to show how the decay of fluctuations is described within the framework of linearised hydrodynamics and, secondly, to obtain explicit expressions for the macroscopic transport coefficients in terms of microscopic quantities. The hydrodynamic approach is valid only on scales of length and time much larger than those characteristic of the molecular level, but we show how the gap between the microscopic and macroscopic descriptions can be bridged by an essentially phenomenological extrapolation of the hydrodynamic results to shorter wavelengths and higher frequencies. The same problem is taken up in a more systematic way in Chapter 9.

8.1 THERMAL FLUCTUATIONS AT LONG WAVELENGTHS AND LOW FREQUENCIES

We have seen in Section 4.1 that the microscopic structure of a liquid is revealed experimentally by the scattering of radiation of wavelength comparable with the interparticle spacing. Examination of a typical pair distribution function, such as the one pictured in Figure 2.1, shows that positional correlations decay rapidly in space and are negligibly small at separations beyond a few molecular diameters. From a static point of view, therefore, a fluid behaves, for longer wavelengths, essentially as a continuum. When discussing the dynamics, however, it is necessary to consider simultaneously the scales both of length and time. In keeping with traditional kinetic theory it is conventional to compare wavelengths with the mean free path l_c and times with the mean collision time τ_c. The wavenumber–frequency plane may then be divided into three parts. The region in which $kl_c \ll 1,\ \omega\tau_c \ll 1$ corresponds to the *hydrodynamic* regime, in which the behaviour of the fluid is described by the phenomenological equations of macroscopic fluid mechanics. The range of intermediate wavenumbers and frequencies ($kl_c \approx 1, \omega\tau_c \approx 1$) forms the *kinetic* regime, where allowance must be made for the molecular structure of the fluid and a treatment based on the microscopic equations of motion is required. Finally, the region where $kl_c \gg 1,\ \omega\tau_c \gg 1$ represents the *free-particle* regime; here the distances and times involved are so short that the particles move almost independently of each other.

In this chapter we shall be concerned mostly with the hydrodynamic regime, where the local properties of the fluid vary slowly on microscopic scales of length and time. The set of *hydrodynamic variables* or *hydrodynamic fields* include the densities of mass (or particle number), energy and momentum; these are closely related to the conserved microscopic variables introduced in Section 7.4. Like their microscopic counterparts, the conserved hydrodynamic variables satisfy continuity equations of the form (7.4.3), which express the conservation of matter, energy and momentum. In addition, there exist certain *constitutive relations* between the fluxes (or currents) and gradients of the local variables, expressed in terms of phenomenological *transport coefficients*. Fick's law of diffusion and Fourier's law of heat transport are two of the more familiar examples of a constitutive relation.

One of the main tasks of the present chapter is to obtain microscopic expressions for the transport coefficients that are similar in structure to the formula (7.7.10) already derived for the electrical conductivity of an ionic fluid. This is achieved by calculating the *hydrodynamic limit* of the appropriate time-correlation function. To understand what is involved in such a calculation it is first necessary to clarify the relationship between hydrodynamic and microscopic dynamical variables. As an example, consider the local density. The microscopic particle density $\rho(\mathbf{r}, t)$ is defined by (7.4.5); its integral over all volume is equal to N, the total number of particles in the system. The hydrodynamic local density $\bar{\rho}(\mathbf{r}, t)$ is obtained by averaging the microscopic density over a subvolume v around the point $\mathbf{r}$ that is macroscopically small but still sufficiently large to ensure that the relative fluctuation in the number of particles inside v is negligible. Then

$$\bar{\rho}(\mathbf{r}, t) = \frac{1}{v} \int_v \rho(\mathbf{r}' - \mathbf{r}, t)\, \mathrm{d}\mathbf{r}' \tag{8.1.1}$$

Strictly speaking, the definition of $\bar{\rho}(\mathbf{r}, t)$ also requires a smoothing or "coarse graining" in time. This can be realised by averaging (8.1.1) over a time interval that is short on a macroscopic scale but long in comparison with the mean collision time. In practice, however, smoothing in time is already achieved by (8.1.1) if the subvolume is sufficiently large. The Fourier components of the hydrodynamic density are defined as

$$\bar{\rho}_{\mathbf{k}}(t) = \int \bar{\rho}(\mathbf{r}, t) \exp(-i\mathbf{k} \cdot \mathbf{r})\, \mathrm{d}\mathbf{r} \tag{8.1.2}$$

where the wavevector $\mathbf{k}$ must be such that k is less than about $2\pi/v^{1/3}$. The corresponding density autocorrelation function is then defined as in (7.4.20), except that the Fourier components of the microscopic density are replaced by $\bar{\rho}_{\mathbf{k}}$. Since we are now working at the macroscopic level, the average to be taken is not an ensemble average, but an average over initial conditions, weighted by the probability density of thermodynamic fluctuation theory (see Appendix A). By forming such an average, we are implicitly invoking the hypothesis of *local thermodynamic equilibrium*. In other words, we are assuming that although the hydrodynamic densities vary over macroscopic lengths and times, the fluid contained in each of the subvolumes is in a state of thermodynamic equilibrium, and that the local density, pressure and temperature satisfy the usual relations of equilibrium thermodynamics. These assumptions are particularly plausible at high densities, since in that case local equilibrium is rapidly brought about by collisions between particles.

Once the calculation we have described in words has been carried out, the relations of interest are obtained by supposing that in the limit of long wavelengths ($\lambda \gg l_c$) and long times ($t \gg \tau_c$) or, equivalently, of small wavenumbers and low frequencies, correlation functions derived from the hydrodynamic equations are identical to the correlation functions of the corresponding microscopic variables. This intuitively appealing hypothesis, which is due to Onsager, can be justified on the basis of the fluctuation–dissipation theorem discussed in Section 7.6. In the example of the density autocorrelation function the assumption can be expressed by the statement that

$$\left\langle \rho_{\mathbf{k}}(t)\rho_{-\mathbf{k}} \right\rangle \sim \left\langle \bar{\rho}_{\mathbf{k}}(t)\bar{\rho}_{-\mathbf{k}} \right\rangle, \quad kl_c \ll 1,\ t/\tau_c \gg 1 \tag{8.1.3}$$

with the qualification, explained above, that the meaning of the angular brackets is different for the two correlation functions. As the sections that follow are concerned almost exclusively with the calculation of correlation functions of hydrodynamic variables, no ambiguity is introduced by dropping the bar we have used to distinguish the latter from the corresponding microscopic quantities.

One important implication of the assumption of local thermodynamic equilibrium is that the Maxwell distribution of velocities applies at the local level. The local velocity is defined via the relation

$$\mathbf{p}(\mathbf{r}, t) = \rho_m(\mathbf{r}, t)\mathbf{u}(\mathbf{r}, t) \tag{8.1.4}$$

where $\mathbf{p}(\mathbf{r}, t)$ is the momentum density and $\rho_m(\mathbf{r}, t) = m\rho(\mathbf{r}, t)$ is the mass density (we assume that the fluid contains only one component). The single-particle distribution function is now a function of $\mathbf{r}$ and t and (2.1.26) is replaced by

$$f_{\text{l.e.}}(\mathbf{u}, \mathbf{r}; t) = \rho(\mathbf{r}, t)\left(\frac{m}{2\pi k_{\text{B}} T(\mathbf{r}, t)}\right)^{3/2} \exp\left(\frac{-m|\mathbf{u} - \mathbf{u}(\mathbf{r}, t)|^2}{2k_{\text{B}} T(\mathbf{r}, t)}\right) \tag{8.1.5}$$

where $T(\mathbf{r}, t)$ is the local temperature. The function $f_{\text{l.e.}}(\mathbf{u}, \mathbf{r}; t)$ is called the "local-equilibrium" Maxwell distribution.

8.2 SPACE-DEPENDENT SELF MOTION

As an illustration of the general procedure described in the previous section, we first consider the relatively simple problem of the diffusion of tagged particles. If the tagged particles are physically identical to the other particles in the fluid, and if their concentration is sufficiently low that their mutual interactions can be ignored, the problem is equivalent to that of single-particle motion as described by the self part of the van Hove correlation function $G_{\text{s}}(\mathbf{r}, t)$ (see Section 7.4). The macroscopic tagged-particle density $\rho^{(s)}(\mathbf{r}, t)$ and current $\mathbf{j}^{(s)}(\mathbf{r}, t)$ satisfy a continuity equation of the form

$$\frac{\partial \rho^{(s)}(\mathbf{r}, t)}{\partial t} + \nabla \cdot \mathbf{j}^{(s)}(\mathbf{r}, t) = 0 \tag{8.2.1}$$

and the corresponding constitutive equation is provided by Fick's law:

$$\mathbf{j}^{(s)}(\mathbf{r},t) = -D\nabla\rho^{(s)}(\mathbf{r},t) \tag{8.2.2}$$

where the interdiffusion constant D is in this case the same as the self-diffusion constant. Combination of (8.2.1) and (8.2.2) yields the *diffusion equation*:

$$\frac{\partial\rho^{(s)}(\mathbf{r},t)}{\partial t} = D\nabla^2\rho^{(s)}(\mathbf{r},t) \tag{8.2.3}$$

or, in reciprocal space:

$$\frac{\partial\rho_{\mathbf{k}}^{(s)}(t)}{\partial t} = -Dk^2\rho_{\mathbf{k}}^{(s)}(t) \tag{8.2.4}$$

Equation (8.2.4) can be integrated immediately to give

$$\rho_{\mathbf{k}}^{(s)}(t) = \rho_{\mathbf{k}}^{(s)}\exp\bigl(-Dk^2t\bigr) \tag{8.2.5}$$

where $\rho_{\mathbf{k}}^{(s)}$ is a Fourier component of the tagged-particle density at $t = 0$. If we multiply both sides of (8.2.5) by $\rho_{-\mathbf{k}}^{(s)}$ and take the thermal average, we find that the normalised autocorrelation function is

$$\frac{1}{n}\bigl\langle\rho_{\mathbf{k}}^{(s)}(t)\rho_{-\mathbf{k}}^{(s)}\bigr\rangle = \frac{1}{n}\bigl\langle\rho_{\mathbf{k}}^{(s)}\rho_{-\mathbf{k}}^{(s)}\bigr\rangle\exp\bigl(-Dk^2t\bigr) = \exp\bigl(-Dk^2t\bigr) \tag{8.2.6}$$

where n is the total number of tagged particles. Here we have used the fact that because the concentration of tagged particles is low, their coordinates are mutually uncorrelated. It then follows from the general hypothesis discussed in Section 8.1 that in the hydrodynamic limit the self part of the density autocorrelation function (7.4.21), i.e. the self intermediate scattering function defined by (7.5.12), behaves as

$$F_{\mathrm{s}}(k,t) \sim \exp\bigl(-Dk^2t\bigr), \quad kl_c \ll 1,\ t/\tau_c \gg 1 \tag{8.2.7}$$

The long-wavelength, low-frequency limit of the van Hove self correlation function is the spatial Fourier transform of (8.2.7):

$$G_{\mathrm{s}}(r,t) = \frac{1}{(4\pi Dt)^{3/2}}\exp\bigl(-r^2/4Dt\bigr) \tag{8.2.8}$$

In the same limit the self dynamic structure factor is

$$S_{\mathrm{s}}(k,\omega) = \frac{1}{\pi}\frac{Dk^2}{\omega^2 + (Dk^2)^2} \tag{8.2.9}$$

Equation (8.2.9) represents a single, lorentzian curve centred at $\omega = 0$ with a width at half-height equal to $2Dk^2$. A spectrum of this type is typical of any diffusive process described

by an equation similar to (8.2.3). Alternatively, the structure of the Laplace transform of (8.2.7), i.e.

$$\widetilde{F}_s(k,z) = \frac{1}{-iz + Dk^2} \tag{8.2.10}$$

shows that a diffusive process is characterised by a purely imaginary pole at $z = -iDk^2$. It should be emphasised again that the simple result expressed by (8.2.9) is valid only for $kl_c \ll 1,\ \omega\tau_c \ll 1$. Its breakdown at high frequencies is reflected in the fact that the even frequency moments (beyond zeroth order) of $S_s(k,\omega)$ are all infinite. Note also that the transport coefficient D is related to the behaviour of $S_s(k,\omega)$ in the limit $k,\ \omega \to 0$. From (8.2.9) we see that

$$D = \lim_{\omega\to 0}\lim_{k\to 0}\frac{\omega^2}{k^2}\pi S_s(k\cdot\omega) \tag{8.2.11}$$

where it is crucial that the limits are taken in the correct order, i.e. $k \to 0$ before $\omega \to 0$. In principle, (8.2.11) provides a means of determining D from the results of inelastic neutron-scattering experiments.

Equations (7.5.16) and (8.2.8) show that the van Hove self correlation function is a gaussian function of r both for $t \to 0$ (free-particle behaviour) and $t \to \infty$ (the hydrodynamic limit); it is therefore tempting to suppose that the function is gaussian at all times. To study this point in more detail we write $G_s(r,t)$ as a generalised gaussian function of r in the form

$$G_s(r,t) = \left(\frac{\alpha(t)}{\pi}\right)^{3/2}\exp\bigl[-\alpha(t)r^2\bigr] \tag{8.2.12}$$

where $\alpha(t)$ is a function of t but not of r; the hydrodynamic limit corresponds to taking $\alpha(t) = 1/4Dt$ and the ideal-gas model to $\alpha(t) = m/2k_BTt^2$. The mean-square displacement of tagged particles after a time t is the second moment of $G_s(r,t)$, i.e.

$$\bigl\langle r^2(t)\bigr\rangle \equiv \bigl\langle\bigl|\mathbf{r}(t) - \mathbf{r}(0)\bigr|^2\bigr\rangle = \int r^2 G_s(r,t)\,\mathrm{d}\mathbf{r} \tag{8.2.13}$$

and is therefore related to the unknown function $\alpha(t)$ by $\langle r^2(t)\rangle = 3/2\alpha(t)$. If we insert this result in (8.2.12) and take the Fourier transform, we find that in the gaussian approximation the self intermediate scattering function has the form

$$F_s(k,t) = \exp\left(-\frac{k^2}{6}\bigl\langle r^2(t)\bigr\rangle\right) \tag{8.2.14}$$

Systematic corrections to the gaussian approximation can be obtained from a cumulant expansion of $F_s(k,t)$ in powers of k^2. Comparison with molecular-dynamics results for argon-like liquids shows that in the intermediate range of k between the free-particle and hydrodynamic regimes the first correction (of order k^4) to (8.2.14) is typically 10% or less and positive; corrections of higher order are even smaller.[1]

The Einstein expression for the long-time limit of the mean-square displacement of a tagged particle is a direct consequence of the hydrodynamic result for $G_s(r,t)$; substitution

of (8.2.8) into the definition (8.2.13) leads immediately to (7.2.3). Since the mean-square displacement is also related to the velocity autocorrelation function through (7.2.6), there is a close connection between the functions $G_s(r,t)$ (or $F_s(k,t)$) and $Z(t)$. In fact, in the gaussian approximation represented by (8.2.14), $F_s(k,t)$ is entirely determined by $Z(t)$ and vice versa; more generally, only the second of these statements is true. To see the significance of this connection we return briefly to the description of the system in terms of microscopic variables. If we define the Fourier components of the microscopic current associated with a tagged particle i having velocity $\mathbf{u}_i$ as

$$\mathbf{j}_{\mathbf{k}i}(t) = \mathbf{u}_i(t)\exp\bigl[-i\mathbf{k}\cdot\mathbf{r}_i(t)\bigr] \tag{8.2.15}$$

and the self-current autocorrelation function as

$$C_s(k,t) = \bigl\langle \mathbf{k}\cdot\mathbf{j}_{\mathbf{k}i}(t)\mathbf{k}\cdot\mathbf{j}_{-\mathbf{k}i}\bigr\rangle \tag{8.2.16}$$

it is clear that

$$Z(t) = \bigl\langle u_{iz}(t)u_{iz}\bigr\rangle = \lim_{k\to 0}\frac{1}{k^2}C_s(k,t) = -\lim_{k\to 0}\frac{1}{k^2}\frac{\mathrm{d}^2}{\mathrm{d}t^2}F_s(k,t) \tag{8.2.17}$$

where we have chosen $\mathbf{k}$ to lie along the z-axis and used the single-particle version of (7.4.26). The relation between the corresponding power spectra is

$$Z(\omega) = \frac{\omega^2}{2\pi}\lim_{k\to 0}\frac{1}{k^2}\int_{-\infty}^{\infty}F_s(k,t)\exp(i\omega t)\,\mathrm{d}t = \omega^2\lim_{k\to 0}\frac{S_s(k,\omega)}{k^2} \tag{8.2.18}$$

Equation (8.2.18) may be regarded as a generalisation of (8.2.11) to non-zero frequencies in which $Z(\omega)$ appears as a frequency-dependent diffusion coefficient; it also provides a possible route to an experimental determination of the velocity autocorrelation function.

The relationship between $Z(t)$ and $F_s(k,t)$ (or $C_s(k,t)$) is further reflected in the short-time expansions of these functions. By analogy with (7.4.31) the expansion of $C_s(k,t)$ in powers of t can be written as

$$C_s(k,t) = \omega_0^2\left(1 - \omega_{1s}^2\frac{t^2}{2!} + \cdots\right) \tag{8.2.19}$$

From the general result (7.1.23) and the continuity equation (8.2.1) it follows that

$$\begin{aligned}\omega_0^2\omega_{1s}^2 &= -\bigl\langle \mathbf{k}\cdot\dot{\mathbf{j}}_{\mathbf{k}i}\mathbf{k}\cdot\dot{\mathbf{j}}_{-\mathbf{k}i}\bigr\rangle = \langle\ddot{\rho}_{\mathbf{k}i}\ddot{\rho}_{-\mathbf{k}i}\rangle \\ &= k^4\bigl\langle u_{iz}^4\bigr\rangle + k^2\bigl\langle \dot{u}_{iz}^2\bigr\rangle = 3\omega_0^4 + \bigl(k^2/m^2\bigr)\bigl\langle F_{iz}^2\bigr\rangle\end{aligned} \tag{8.2.20}$$

and hence, from the definition (7.2.9), that

$$\omega_{1s}^2 = 3\omega_0^2 + \Omega_0^2 \tag{8.2.21}$$

The next term (of order t^4) in the Taylor expansion of $C_s(k,t)$ involves integrals over the triplet distribution function. Short-time expansions such as (8.2.19) are useful in extending the validity of hydrodynamic results to microscopic scales of length and time.

8.3 THE NAVIER–STOKES EQUATION AND HYDRODYNAMIC COLLECTIVE MODES

We turn now to the problem of describing the decay of long-wavelength fluctuations in the collective dynamical variables. For a one-component fluid the macroscopic local densities associated with the conserved variables are the number density $\rho(\mathbf{r},t)$, energy density $e(\mathbf{r},t)$ and momentum density $\mathbf{p}(\mathbf{r},t)$. The conservation laws for the local densities have the form

$$m\frac{\partial}{\partial t}\rho(\mathbf{r},t)+\nabla\cdot\mathbf{p}(\mathbf{r},t)=0 \tag{8.3.1}$$

$$\frac{\partial}{\partial t}e(\mathbf{r},t)+\nabla\cdot\mathbf{J}^e(\mathbf{r},t)=0 \tag{8.3.2}$$

$$\frac{\partial}{\partial t}\mathbf{p}(\mathbf{r},t)+\nabla\cdot\boldsymbol{\Pi}(\mathbf{r},t)=0 \tag{8.3.3}$$

where $\mathbf{J}^e$ is the energy current and $\boldsymbol{\Pi}$ is the momentum current or *stress tensor*. These equations must be supplemented by two constitutive relations in which $\mathbf{J}^e$ and $\boldsymbol{\Pi}$ are expressed in terms of quantities representing dissipative processes in the fluid. We choose a frame of reference in which the mean velocity of the fluid is zero, i.e. $\langle\mathbf{u}(\mathbf{r},t)\rangle=0$, and assume that the local deviations of the hydrodynamic variables from their average values are small. The equations may then be linearised with respect to the deviations. We consider in turn each of the three conservation laws.

Conservation of particle number. Equation (8.3.1) is easily dealt with. The assumption that the local deviation in number density is small means that the momentum density can be written as

$$\mathbf{p}(\mathbf{r},t)=m\big[\rho+\delta\rho(\mathbf{r},t)\big]\mathbf{u}(\mathbf{r},t)\approx m\rho\mathbf{u}(\mathbf{r},t)\equiv m\mathbf{j}(\mathbf{r},t) \tag{8.3.4}$$

which also serves as the definition of the local particle current $\mathbf{j}(\mathbf{r},t)$. With this approximation, (8.3.1) becomes

$$\frac{\partial}{\partial t}\delta\rho(\mathbf{r},t)+\nabla\cdot\mathbf{j}(\mathbf{r},t)=0 \tag{8.3.5}$$

Conservation of energy. The macroscopic energy current $\mathbf{J}^e$ is defined as

$$\mathbf{J}^e(\mathbf{r},t)=(e+P)\mathbf{u}(\mathbf{r},t)-\lambda\nabla T(\mathbf{r},t) \tag{8.3.6}$$

where $e=U/V$ is the equilibrium energy density, λ is the thermal conductivity and $T(\mathbf{r},t)$ is the local temperature already introduced in (8.1.5); terms corresponding to viscous heating have been omitted, since these are quadratic in the local velocity. Equations (8.3.2),

(8.3.5) and (8.3.6) can now be combined to give the *energy equation*, i.e.

$$\frac{\partial}{\partial t}\delta q(\mathbf{r},t) - \lambda\nabla^2\delta T(\mathbf{r},t) = 0 \tag{8.3.7}$$

where $\delta q(\mathbf{r},t)$ is the fluctuation in a quantity

$$q(\mathbf{r},t) = e(\mathbf{r},t) - \left(\frac{e+P}{\rho}\right)\rho(\mathbf{r},t) \tag{8.3.8}$$

which can be interpreted as a density of heat energy. If the number of particles is held constant, the entropy change of the system in an infinitesimal process is $T\,\mathrm{d}S = \mathrm{d}U + P\,\mathrm{d}V$. Hence

$$T\,\mathrm{d}S = \mathrm{d}(eV) + P\,\mathrm{d}V = V\,\mathrm{d}e - \frac{eV}{\rho}\,\mathrm{d}\rho - \frac{PV}{\rho}\,\mathrm{d}\rho = V\,\mathrm{d}q \tag{8.3.9}$$

A change in q is therefore equal to the heat lost or gained by the system per unit volume when the change is carried out reversibly and $\delta q(\mathbf{r},t)$ is related to the change in entropy density $s(\mathbf{r},t)$ by

$$\delta q(\mathbf{r},t) = T\delta s(\mathbf{r},t) \tag{8.3.10}$$

If we invoke the hypothesis of local thermodynamic equilibrium, the deviation of a local thermodynamic variable such as $s(\mathbf{r},t)$ from its average value can be expressed in terms of a set of statistically independent quantities. We choose as independent variables the density and temperature (see Appendix A) and expand $q(\mathbf{r},t)$ to first order in the deviations $\delta\rho(\mathbf{r},t)$ and $\delta T(\mathbf{r},t)$. Then, from (8.3.10), and remembering that N is fixed:

$$\begin{aligned}\delta q(\mathbf{r},t) &= \frac{T}{V}\left(\frac{\partial S}{\partial\rho}\right)_T \delta\rho(\mathbf{r},t) + \frac{T}{V}\left(\frac{\partial S}{\partial T}\right)_\rho \delta T(\mathbf{r},t)\\ &= -\frac{T\beta_V}{\rho}\,\delta\rho(\mathbf{r},t) + \rho c_V \delta T(\mathbf{r},t)\end{aligned} \tag{8.3.11}$$

where

$$\beta_V = \left(\frac{\partial P}{\partial T}\right)_\rho = -\rho\left(\frac{\partial(S/V)}{\partial\rho}\right)_T \tag{8.3.12}$$

is the thermal pressure coefficient, c_V is the heat capacity per particle at constant volume and use has been made of the Maxwell relation $(\partial S/\partial V)_T = (\partial P/\partial T)_V$. If we now substitute (8.3.11) in (8.3.7), eliminate $(\partial/\partial t)\rho(\mathbf{r},t)$ with the help of (8.3.5) and divide through by ρc_V, the energy equation becomes

$$\left(\frac{\partial}{\partial t} - a\nabla^2\right)\delta T(\mathbf{r},t) + \frac{T\beta_V}{\rho^2 c_V}\boldsymbol{\nabla}\cdot\mathbf{j}(\mathbf{r},t) = 0 \tag{8.3.13}$$

where

$$a = \frac{\lambda}{\rho c_V} \tag{8.3.14}$$

Conservation of momentum. The stress tensor $\boldsymbol{\Pi}$ in (8.3.3) is given macroscopically by

$$\begin{aligned}\Pi^{\alpha\beta}(\mathbf{r},t) = \delta_{\alpha\beta}P(\mathbf{r},t) - \eta\left(\frac{\partial u_\alpha(\mathbf{r},t)}{\partial r_\beta} + \frac{\partial u_\beta(\mathbf{r},t)}{\partial r_\alpha}\right) \\ + \delta_{\alpha\beta}\left(\tfrac{2}{3}\eta - \zeta\right)\boldsymbol{\nabla}\cdot\mathbf{u}(\mathbf{r},t)\end{aligned} \tag{8.3.15}$$

where $P(\mathbf{r},t)$ is the local pressure, η is the shear viscosity, ζ is the bulk viscosity and the bracketed quantity in the second term on the right-hand side is the rate-of-strain tensor.[2] Substitution of (8.3.15) in (8.3.3) and use of (8.3.5) leads to the Navier–Stokes equation in its linearised form:

$$\frac{\partial}{\partial t}\mathbf{j}(\mathbf{r},t) + \frac{1}{m}\boldsymbol{\nabla}P(\mathbf{r},t) - \nu\nabla^2\mathbf{j}(\mathbf{r},t) - \frac{\frac{1}{3}\eta+\zeta}{\rho m}\boldsymbol{\nabla}\boldsymbol{\nabla}\cdot\mathbf{j}(\mathbf{r},t) = 0 \tag{8.3.16}$$

where

$$\nu = \frac{\eta}{\rho m} \tag{8.3.17}$$

is the kinematic shear viscosity. To first order in $\delta\rho(\mathbf{r},t)$ and $\delta T(\mathbf{r},t)$ the fluctuation in local pressure is

$$\begin{aligned}\delta P(\mathbf{r},t) &= \left(\frac{\partial P}{\partial \rho}\right)_T \delta\rho(\mathbf{r},t) + \left(\frac{\partial P}{\partial T}\right)_\rho \delta T(\mathbf{r},t) \\ &= \frac{1}{\rho\chi_T}\,\delta\rho(\mathbf{r},t) + \beta_V \delta T(\mathbf{r},t)\end{aligned} \tag{8.3.18}$$

where χ_T is the isothermal compressibility (2.4.16). The Navier–Stokes equation can therefore be rewritten as

$$\frac{1}{\rho m\chi_T}\boldsymbol{\nabla}\delta\rho(\mathbf{r},t) + \frac{\beta_V}{m}\boldsymbol{\nabla}\delta T(\mathbf{r},t) + \left(\frac{\partial}{\partial t} - \nu\nabla^2 - \frac{\frac{1}{3}\eta+\zeta}{\rho m}\boldsymbol{\nabla}\boldsymbol{\nabla}\cdot\right)\mathbf{j}(\mathbf{r},t) = 0 \tag{8.3.19}$$

Equations (8.3.5), (8.3.13) and (8.3.19) form a closed set of linear equations for the variables $\delta\rho(\mathbf{r},t)$, $\delta T(\mathbf{r},t)$ and $\mathbf{j}(\mathbf{r},t)$. These are readily solved by taking the double transforms with respect to space (Fourier) and time (Laplace) to give

$$-iz\tilde{\rho}_{\mathbf{k}}(z) + i\mathbf{k}\cdot\tilde{\mathbf{j}}_{\mathbf{k}}(z) = \rho_{\mathbf{k}} \tag{8.3.20}$$

$$\left(-iz + ak^2\right)\widetilde{T}_{\mathbf{k}}(z) + \frac{T\beta_V}{\rho^2 c_V} i\mathbf{k}\cdot\tilde{\mathbf{j}}_{\mathbf{k}}(z) = T_{\mathbf{k}} \tag{8.3.21}$$

$$\frac{1}{\rho m \chi_T} i\mathbf{k}\tilde{\rho}_{\mathbf{k}}(z) + \frac{\beta_V}{m} i\mathbf{k}\widetilde{T}_{\mathbf{k}}(z) + \left(-iz + \nu k^2 + \frac{\frac{1}{3}\eta + \zeta}{\rho m}\mathbf{k}\mathbf{k}\cdot\right)\tilde{\mathbf{j}}_{\mathbf{k}}(z) = \mathbf{j}_{\mathbf{k}} \tag{8.3.22}$$

where, for example:

$$\tilde{\rho}_{\mathbf{k}}(z) = \int_0^\infty \mathrm{d}t\ \exp(izt) \int \delta\rho(\mathbf{r}, t) \exp(-i\mathbf{k}\cdot\mathbf{r})\, \mathrm{d}\mathbf{r} \tag{8.3.23}$$

and $\rho_{\mathbf{k}}$, $T_{\mathbf{k}}$ and $\mathbf{j}_{\mathbf{k}}$ are the spatial Fourier components at $t = 0$. We now separate the components of the current $\mathbf{j}_{\mathbf{k}}$ into their longitudinal and transverse parts. Taking $\mathbf{k}$ along the z-axis, we rewrite (8.3.22) as

$$\frac{1}{\rho m \chi_T} ik\tilde{\rho}_{\mathbf{k}}(z) + \frac{\beta_V}{m} ik\widetilde{T}_{\mathbf{k}}(z) + \left(-iz + bk^2\right)\tilde{j}^z_{\mathbf{k}}(z) = j^z_{\mathbf{k}} \tag{8.3.24a}$$

$$\left(-iz + \nu k^2\right)\tilde{j}^\alpha_{\mathbf{k}} = j^\alpha_{\mathbf{k}}, \quad \alpha = x, y \tag{8.3.24b}$$

where

$$b = \frac{\frac{4}{3}\eta + \zeta}{\rho m} \tag{8.3.25}$$

is the kinematic longitudinal viscosity.

Equations (8.3.20), (8.3.21) and (8.3.24) are conveniently summarised in matrix form:

$$\begin{pmatrix} -iz & 0 & ik & 0 & 0 \\ 0 & -iz + ak^2 & \dfrac{T\beta_V ik}{\rho^2 c_V} & 0 & 0 \\ \dfrac{ik}{\rho m \chi_T} & \dfrac{\beta_V ik}{m} & -iz + bk^2 & 0 & 0 \\ 0 & 0 & 0 & -iz + \nu k^2 & 0 \\ 0 & 0 & 0 & 0 & -iz + \nu k^2 \end{pmatrix} \begin{pmatrix} \tilde{\rho}_{\mathbf{k}}(z) \\ \widetilde{T}_{\mathbf{k}}(z) \\ \tilde{j}^z_{\mathbf{k}}(z) \\ \tilde{j}^x_{\mathbf{k}}(z) \\ \tilde{j}^y_{\mathbf{k}}(z) \end{pmatrix} = \begin{pmatrix} \rho_{\mathbf{k}} \\ T_{\mathbf{k}} \\ j^z_{\mathbf{k}} \\ j^x_{\mathbf{k}} \\ j^y_{\mathbf{k}} \end{pmatrix} \tag{8.3.26}$$

The matrix of coefficients in (8.3.26) is called the *hydrodynamic matrix*. Its block-diagonal structure shows that the transverse-current fluctuations are completely decoupled from fluctuations in the other, longitudinal variables. The determinant of the hydrodynamic matrix therefore factorises into the product of purely longitudinal (l) and purely transverse (t) parts, i.e.

$$D(k, z) = D_l(k, z) D_t(k, z) \tag{8.3.27}$$

with

$$D_l(k, z) = -iz\left(-iz + ak^2\right)\left(-iz + bk^2\right) + \left(-iz + ak^2\right)\frac{k^2}{\rho m \chi_T} - iz\frac{T\beta_V^2 k^2}{\rho^2 m c_V} \tag{8.3.28}$$

and

$$D_t(k,z) = \left(-iz + \nu k^2\right)^2 \tag{8.3.29}$$

The dependence of frequency on wavenumber or *dispersion relation* for the collective modes is determined by the poles of the inverse of the hydrodynamic matrix and hence by the complex roots of the equation

$$D(k,z) = 0 \tag{8.3.30}$$

The factorisation in (8.3.27) shows that (8.3.30) has a double root associated with the two transverse modes, namely

$$z = -i\nu k^2 \tag{8.3.31}$$

while the complex frequencies corresponding to longitudinal modes are obtained as the solution to the cubic equation

$$iz^3 - z^2(a+b)k^2 - iz\left(abk^2 + c_s^2\right)k^2 + (a/\gamma)c_s^2 k^4 = 0 \tag{8.3.32}$$

where $\gamma = c_P/c_V$ is the ratio of specific heats, c_s is the adiabatic speed of sound, given by

$$c_s^2 = \frac{\gamma}{\rho m \chi_T} \tag{8.3.33}$$

and use has been made of the thermodynamic relation[3]

$$c_P = c_V + \frac{T\chi_T \beta_V^2}{\rho} \tag{8.3.34}$$

Since the hydrodynamic calculation is valid only in the long-wavelength limit, it is sufficient to calculate the complex frequencies to order k^2. The algebra is simplified by introducing the reduced variables $s = z/c_s k$; it is then straightforward to show[4] that the approximate solution to (8.3.32) is

$$z_0 = -iD_T k^2 \tag{8.3.35a}$$

$$z_\pm = \pm c_s k - i\Gamma k^2 \tag{8.3.35b}$$

where

$$D_T = \frac{a}{\gamma} = \frac{\lambda}{\rho c_P} \tag{8.3.36}$$

is the thermal diffusivity and

$$\Gamma = a(\gamma - 1)/2\gamma + b/2 \tag{8.3.37}$$

is the sound attenuation coefficient. The imaginary roots in (8.3.31) and (8.3.35a) represent diffusive processes of the type already discussed in the preceding section, and the pair of complex roots in (8.3.35b) correspond to propagating sound waves, as we shall see in Section 8.5.

8.4 TRANSVERSE-CURRENT CORRELATIONS

Equation (8.3.24b) shows that in the time domain the hydrodynamic behaviour of the transverse-current fluctuations is governed by a first-order differential equation of the form

$$\frac{\partial}{\partial t} j^x_{\mathbf{k}}(t) = -\nu k^2 j^x_{\mathbf{k}}(t) \tag{8.4.1}$$

This result has precisely the same structure as the diffusion equation (8.2.4) and the kinematic shear viscosity has the same dimensions as the self-diffusion coefficient, but is typically two orders of magnitude larger than D for, say, an argon-like liquid near its triple point. If we multiply through (8.4.1) by $j^x_{-\mathbf{k}}$ and take the thermal average we find that the transverse current autocorrelation function satisfies the equation

$$\frac{\partial}{\partial t} C_t(k,t) + \nu k^2 C_t(k,t) = 0 \tag{8.4.2}$$

Equation (8.4.2) is easily solved to give

$$C_t(k,t) = C_t(k,0)\exp\bigl(-\nu k^2 t\bigr) = \omega_0^2 \exp\bigl(-\nu k^2 t\bigr) \tag{8.4.3}$$

where ω_0 is the frequency defined by (7.4.29). The exponential decay in (8.4.3) is typical of a diffusive process (see Section 8.2).

The diffusive behaviour of the hydrodynamic "shear" mode is also apparent in the fact that the Laplace transform of $C_t(k,t)$ has a purely imaginary pole corresponding to the root (8.3.31) of $D(k,z)$:

$$\widetilde{C}_t(k,z) = \frac{\omega_0^2}{-iz + \nu k^2} \tag{8.4.4}$$

Let $z = \omega + i\varepsilon$ approach the real axis from above ($\varepsilon \to 0+$). Then $\widetilde{C}_t(k,\omega)$ at small k is given approximately by

$$\widetilde{C}_t(k,\omega) = \frac{\omega_0^2}{-i\omega}\left(1 - \frac{\nu k^2}{i\omega}\right)^{-1} \approx \frac{\omega_0^2}{-i\omega}\left(1 + \frac{\nu k^2}{i\omega}\right) \tag{8.4.5}$$

If we substitute for ω_0^2 and recall the definition (8.3.17) of ν, we find that the shear viscosity, which must be real, is related to the long-wavelength, low-frequency behaviour of

$\widetilde{C}_t(k,\omega)$ by

$$\eta = \beta\rho m^2 \lim_{\omega\to 0}\lim_{k\to 0}\frac{\omega^2}{k^4}\mathrm{Re}\,\widetilde{C}_t(k,\omega)$$
$$= \pi\beta\rho m^2 \lim_{\omega\to 0}\lim_{k\to 0}\frac{\omega^2}{k^4}C_t(k,\omega) \tag{8.4.6}$$

where $C_t(k,\omega)$ is the spectrum of transverse-current fluctuations, i.e. the Fourier transform of $C_t(k,t)$; this result is the analogue of the expression (8.2.11) for the self-diffusion coefficient. From the properties of the Laplace transform and the definition of $C_t(k,t)$ it follows that

$$\frac{k^2}{N}\int_0^\infty \langle \dot{j}^x_{\mathbf{k}}(t)\dot{j}^x_{-\mathbf{k}}\rangle \exp(i\omega t)\,\mathrm{d}t = -\int_0^\infty \frac{\mathrm{d}^2}{\mathrm{d}t^2}C_t(k,t)\exp(i\omega t)\,\mathrm{d}t$$
$$= \omega^2\widetilde{C}_t(k,\omega) - i\omega\omega_0^2 \tag{8.4.7}$$

We may therefore rewrite (8.4.6) as

$$\eta = \frac{\beta m^2}{V}\lim_{\omega\to 0}\lim_{k\to 0}\mathrm{Re}\int_0^\infty \frac{1}{k^2}\langle \dot{j}^x_{\mathbf{k}}(t)\dot{j}^x_{-\mathbf{k}}\rangle \exp(i\omega t)\,\mathrm{d}t \tag{8.4.8}$$

The time derivative of the transverse current can be expressed in terms of the stress tensor via the conservation law (8.3.3). Taking the Fourier transform of (8.3.3), and remembering that $\mathbf{k}$ lies along the z-axis and that $\mathbf{p}(\mathbf{r},t) = m\mathbf{j}(\mathbf{r},t)$, we find that

$$\frac{\partial}{\partial t}j^x_{\mathbf{k}}(t) + \frac{ik}{m}\Pi^{xz}_{\mathbf{k}}(t) = 0 \tag{8.4.9}$$

Combination of (8.4.8) and (8.4.9) shows that the shear viscosity is proportional to the time integral of the autocorrelation function of an off-diagonal element of the stress tensor in the limit $k \to 0$:

$$\eta = \frac{\beta}{V}\int_0^\infty \langle \Pi^{xz}_0(t)\Pi^{xz}_0\rangle \mathrm{d}t \equiv \int_0^\infty \eta(t)\,\mathrm{d}t \tag{8.4.10}$$

In order to relate the shear viscosity to the intermolecular forces it is necessary to have a microscopic expression for the stress tensor. It follows from the definition (7.4.7) of the microscopic particle current that

$$m\frac{\partial}{\partial t}j^\alpha_{\mathbf{k}} = m\sum_{i=1}^N\left(\dot{u}_{i\alpha} - \sum_\beta ik_\beta u_{i\alpha}u_{i\beta}\right)\exp(-i\mathbf{k}\cdot\mathbf{r}_i) \tag{8.4.11}$$

where α, β denote any of x, y or z; the relation to the stress tensor is then established by use of (8.4.9), with $\alpha = x$ and $\beta = z$. To introduce the pair potential $v(r)$ we note that

$\mathbf{r}_{ji} = -\mathbf{r}_{ij}$, and rewrite the first term on the right-hand side of (8.4.11) successively as

$$\begin{aligned} & m\sum_{i=1}^{N} \dot{u}_{i\alpha} \exp(-i\mathbf{k}\cdot\mathbf{r}_i) \\ &= \sum_{i=1}^{N}\sum_{j\neq i}^{N} \frac{r_{ij\alpha}}{|\mathbf{r}_{ij}|} v'(r_{ij}) \exp(-i\mathbf{k}\cdot\mathbf{r}_i) \\ &= \tfrac{1}{2}\sum_{i=1}^{N}\sum_{j\neq i}^{N} \frac{r_{ij\alpha}}{|\mathbf{r}_{ij}|} v'(r_{ij}) \big[\exp(-i\mathbf{k}\cdot\mathbf{r}_i) - \exp(-i\mathbf{k}\cdot\mathbf{r}_j)\big] \\ &= \tfrac{1}{2} ik_\beta \sum_{i=1}^{N}\sum_{j\neq i}^{N} \frac{r_{ij\alpha} r_{ij\beta}}{ik_\beta r_{ij\beta}|\mathbf{r}_{ij}|} v'(r_{ij}) \big[\exp(-i\mathbf{k}\cdot\mathbf{r}_i) - \exp(-i\mathbf{k}\cdot\mathbf{r}_j)\big] \end{aligned} \tag{8.4.12}$$

where $v'(r) \equiv \mathrm{d}v(r)/\mathrm{d}r$; the second step is taken by writing each term in the double sum as half the sum of two equal terms. Introducing a quantity $\Phi_{\mathbf{k}}(\mathbf{r})$ defined as

$$\Phi_{\mathbf{k}}(\mathbf{r}) = r v'(r) \left(\frac{\exp(i\mathbf{k}\cdot\mathbf{r}) - 1}{i\mathbf{k}\cdot\mathbf{r}} \right) \tag{8.4.13}$$

we finally obtain a microscopic expression for $\Pi_{\mathbf{k}}^{\alpha\beta}$ in the form

$$\Pi_{\mathbf{k}}^{\alpha\beta} = \sum_{i=1}^{N} \left(m u_{i\alpha} u_{i\beta} + \tfrac{1}{2} \sum_{j\neq i}^{N} \frac{r_{ij\alpha} r_{ij\beta}}{r_{ij}^2} \Phi_{\mathbf{k}}(\mathbf{r}_{ij}) \right) \exp(-i\mathbf{k}\cdot\mathbf{r}_i) \tag{8.4.14}$$

The Green–Kubo relation for the shear viscosity analogous to (7.2.7) is then obtained by inserting (8.4.14) (taken for $\mathbf{k} = 0$) in (8.4.10). Note that it follows from the virial theorem that

$$\left\langle \Pi_0^{\alpha\alpha} \right\rangle = PV \tag{8.4.15}$$

whereas

$$\left\langle \Pi_0^{\alpha\beta} \right\rangle = 0, \quad \alpha \neq \beta \tag{8.4.16}$$

Equation (8.4.10) is not directly applicable to the hard-sphere fluid because the potential $v(r)$ has a singularity at $r = d$ (the hard-sphere diameter). However, the microscopic expression for the shear viscosity, together with formulae to be derived later for other transport coefficients, can be recast in a form that resembles the Einstein relation (7.2.3) for the self-diffusion coefficient and is valid even for hard spheres. A Green–Kubo formula for a transport coefficient K, including both (7.7.10) (taken for $\omega = 0$) and (8.4.10), can always be written as

$$K = \frac{\beta}{V} \int_0^\infty \left\langle \dot{A}(t) \dot{A} \right\rangle \mathrm{d}t \tag{8.4.17}$$

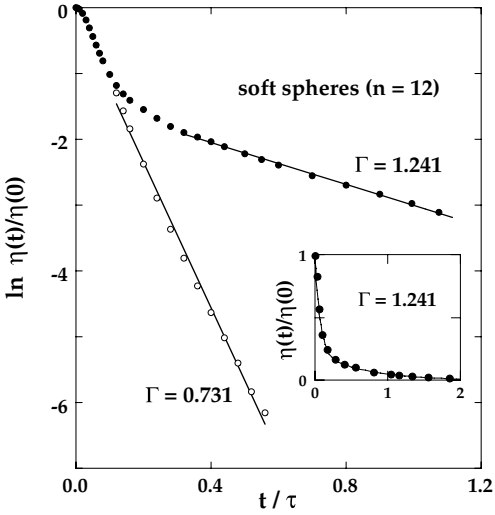

FIG. 8.1. Normalised Green–Kubo integrand for the shear viscosity of a soft-sphere (r^{-12}) fluid at two values of the coupling parameter Γ defined by (5.3.13). The unit of time is $\tau = (m\sigma^2/48\varepsilon)^{1/2}$. The inset shows the results of a two-exponential fit to $\eta(t)$ at the higher value of Γ. Unpublished results of D.M. Heyes.

where A is some microscopic dynamical variable. The argument used to derive (7.2.7) from (7.2.3) can be extended to show that (8.4.17) is equivalent to writing

$$K = \frac{\beta}{V} \lim_{t\to\infty} \frac{1}{2t} \left\langle \left| A(t) - A(0) \right|^2 \right\rangle \tag{8.4.18}$$

which may be regarded as a generalised form of the Einstein relation for D. In the case of the shear viscosity we see from (8.4.8) that the variable $A(t)$ is

$$\begin{aligned} A(t) &= \lim_{k\to 0} \frac{im}{k} j^x_{\mathbf{k}}(t) \\ &= \lim_{k\to 0} \frac{im}{k} \sum_{i=1}^{N} u_{ix}(t)\left[1 - ikr_{iz}(t) + \cdots\right] = m \sum_{i=1}^{N} u_{ix}(t) r_{iz}(t) \end{aligned} \tag{8.4.19}$$

where a frame of reference has been chosen in which the total momentum of the particles (a conserved quantity) is zero. Hence the generalised Einstein relation for the shear viscosity is

$$\eta = \frac{\beta m^2}{V} \lim_{t\to\infty} \frac{1}{2t} \left\langle \left| \sum_{i=1}^{N} \left[u_{ix}(t) r_{iz}(t) - u_{ix}(0) r_{iz}(0) \right] \right|^2 \right\rangle \tag{8.4.20}$$

The quantity Π_0^{xz} in the Green–Kubo formula (8.4.10) is the sum of a kinetic and a potential term. There are consequently three distinct contributions to the shear viscosity:

a purely kinetic term, corresponding to the transport of transverse momentum via the displacement of particles; a purely potential term, arising from the action of the interparticle forces ("collisional" transport); and a cross term. At liquid densities the potential term is much the largest of the three. In Enskog's theory (see Section 7.2) the shear viscosity of the hard-sphere fluid is

$$\frac{\eta_{\mathrm{E}}}{\eta_0} = \frac{2\pi\rho d^3}{3}\left(\frac{1}{y} + 0.8 + 0.761y\right) \tag{8.4.21}$$

where $y = \beta P/\rho - 1 = (2\pi\rho d^3/3)g(d)$ and $\eta_0 = (5/16d^2)(mk_{\mathrm{B}}T/\pi)^{1/2}$ is the limiting, low-density result derived from the Boltzmann equation.[5] The three terms between brackets in (8.4.21) represent, successively, the kinetic, cross and potential contributions; the last of these is dominant close to the fluid–solid transition, where $g(d)$ (the pair distribution function at contact) ≈ 6 and $y \approx 10$. Note that the kinetic contribution scales with $g(d)$ in exactly the same way as the diffusion constant (see Section 2.5); this is not surprising, since diffusion is a purely kinetic phenomenon. Figure 7.3 compares the results of molecular-dynamics calculations of the shear viscosity of the hard-sphere fluid with those obtained from the Enskog expression (8.4.21). Agreement is very good for densities up to $\rho d^3 \approx 0.7$. Near solidification, however, where η increases rapidly with density, Enskog's theory underestimates the shear viscosity by a factor of approximately two. As the same figure also shows, the behaviour of the self-diffusion constant at high densities is the reverse of this. The net result is that the product $D\eta$ calculated from the molecular-dynamics data is roughly constant for ρd^3 greater than about 0.2; at the highest densities its value is within a few percent of that predicted by Stokes's law (7.3.19) with slip boundary conditions. The increase in shear viscosity at high densities is linked numerically to the appearance of a slowly decaying, quasi-exponential tail in the stress-tensor autocorrelation function, colloquially called the "molasses" tail.[6] The effect is not peculiar to hard spheres. For example, a persisting, positive tail is clearly present in the results shown in Figure 8.1 for a soft-sphere (r^{-12}) fluid at a high value of the coupling constant Γ, where $\eta(t)$ is well represented by the sum of two exponentials. At the lower value, corresponding to lower densities or higher temperatures, the tail in $\eta(t)$ – if any – is not perceptible.

8.5 LONGITUDINAL COLLECTIVE MODES

The longitudinal collective modes are those associated with fluctuations in density, temperature and the projection of the particle current along the direction of the wavevector $\mathbf{k}$. It is clear from the structure of the hydrodynamic matrix in (8.3.26) that the variables $\tilde{\rho}_{\mathbf{k}}(z)$, $\widetilde{T}_{\mathbf{k}}(z)$ and $\tilde{j}^z_{\mathbf{k}}(z)$ are coupled to each other. The analysis is therefore more complicated than in the case of the transverse-current fluctuations discussed in Section 8.4. There are three longitudinal modes, corresponding to the roots z_0, z_+ and z_- displayed in (8.3.35). The significance of the different roots is most easily grasped by solving the system of coupled, longitudinal equations represented by (8.3.26) to obtain the hydrodynamic limiting form of the dynamic structure factor $S(k, \omega)$. The solution for $\tilde{\rho}_{\mathbf{k}}(z)$ involves terms proportional to the initial values $\rho_{\mathbf{k}}$, $T_{\mathbf{k}}$ and $j^z_{\mathbf{k}}$. We may omit the term proportional to $j^z_{\mathbf{k}}$ because $\mathbf{k}$ can

always be chosen to make $\mathbf{u}_\mathbf{k}$ (the Fourier transform of the initial local velocity $\mathbf{u}(\mathbf{r}, 0)$) perpendicular to $\mathbf{k}$, thereby ensuring that $j_\mathbf{k}^z = 0$. We can also ignore the term proportional to $T_\mathbf{k}$; this contributes nothing to the final expression for $S(k, \omega)$, since fluctuations in temperature and density are instantaneously uncorrelated, i.e. $\langle T_\mathbf{k} \rho_{-\mathbf{k}} \rangle = 0$ (see Appendix A). With these simplifications the solution for $\tilde{\rho}_\mathbf{k}(z)$ is

$$\frac{\tilde{\rho}_\mathbf{k}(z)}{\rho_\mathbf{k}} = \frac{(-iz + ak^2)(-iz + bk^2) + (\gamma - 1)c_s^2 k^2/\gamma}{D_l(k, z)} \tag{8.5.1}$$

where all quantities are as defined in Section 8.3. Separation of the right-hand side of (8.5.1) into partial fractions shows that on the real axis $\tilde{\rho}_\mathbf{k}$ is given by

$$\begin{aligned}\frac{\tilde{\rho}_\mathbf{k}(\omega)}{\rho_\mathbf{k}} = &\left(\frac{\gamma - 1}{\gamma}\right)\frac{1}{-i\omega + D_T k^2} \\ &+ \frac{1}{2\gamma}\left(\frac{1}{-i\omega + \Gamma k^2 - ic_s k} + \frac{1}{-i\omega + \Gamma k^2 + ic_s k}\right)\end{aligned} \tag{8.5.2}$$

which, via an inverse transform, yields an expression for $\rho_\mathbf{k}(t)$ given by

$$\rho_\mathbf{k}(t) = \rho_\mathbf{k}\left[\left(\frac{\gamma - 1}{\gamma}\right)\exp\left(-D_T k^2 t\right) + \frac{1}{\gamma}\exp\left(-\Gamma k^2 t\right)\cos c_s k t\right] \tag{8.5.3}$$

The form of (8.5.3) shows that the purely imaginary root in (8.3.35a) represents a fluctuation that decays without propagating, the lifetime of the fluctuation being determined by the thermal diffusivity D_T. By contrast, the complex roots correspond to a fluctuation that propagates through the fluid at the speed of sound, eventually decaying through the combined effects of viscosity and thermal conduction. The definition of Γ in (8.3.37) implies that the thermal damping of the sound mode is small when $\gamma \approx 1$, which is the case for many liquid metals. On multiplying through (8.5.3) by $\rho_{-\mathbf{k}}$, dividing by N and taking the thermal average, we obtain an expression for the density autocorrelation function $F(k, t)$; this is easily transformed to give

$$\begin{aligned}S(k, \omega) = \frac{S(k)}{2\pi}&\left[\left(\frac{\gamma - 1}{\gamma}\right)\frac{2D_T k^2}{\omega^2 + (D_T k^2)^2}\right. \\ &\left. + \frac{1}{\gamma}\left(\frac{\Gamma k^2}{(\omega + c_s k)^2 + (\Gamma k^2)^2} + \frac{\Gamma k^2}{(\omega - c_s k)^2 + (\Gamma k^2)^2}\right)\right]\end{aligned} \tag{8.5.4}$$

The spectrum of density fluctuations therefore consists of three components: the *Rayleigh line*, centred at $\omega = 0$, and two *Brillouin lines* at $\omega = \pm c_s k$; a typical spectrum is plotted in Figure 8.2. The two shifted components correspond to propagating sound waves and are analogous to the longitudinal acoustic phonons of a solid, whereas the central line corresponds to the diffusive, thermal mode. The total integrated intensity of the Rayleigh line is

$$\mathcal{I}_R = \frac{\gamma - 1}{\gamma} S(k) \tag{8.5.5}$$

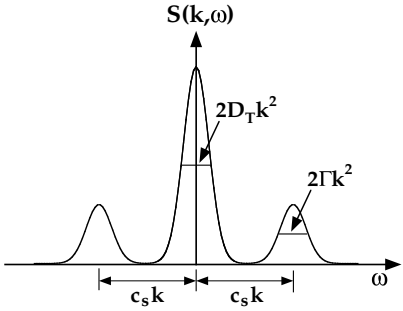

FIG. 8.2. Dynamic structure factor in the hydrodynamic limit. D_T is the thermal diffusivity, Γ is the sound-attenuation coefficient and c_S is the adiabatic speed of sound.

and that of each of the two Brillouin lines is

$$\mathcal{I}_B = \frac{1}{2\gamma} S(k) \tag{8.5.6}$$

Thus

$$\mathcal{I}_R + 2\mathcal{I}_B = S(k) \tag{8.5.7}$$

which is a particular case of the sum rule (7.4.23). The ratio

$$\frac{\mathcal{I}_R}{2\mathcal{I}_B} = \gamma - 1 \tag{8.5.8}$$

is called the Landau–Placzek ratio. As the values of C_P/C_V listed in Table 1.2 suggest, the Landau–Placzek ratio is typically an order of magnitude larger for the rare-gas liquids than for simple liquid metals. In passing from (8.5.1) to (8.5.2) we have, for the sake of simplicity, omitted a non-lorentzian term that in practice makes only a negligibly small, asymmetric correction to the Brillouin lines.

We have chosen to discuss the behaviour of the longitudinal modes in terms of local fluctuations in density and temperature, but it would have been equally appropriate to choose the pressure and entropy as variables, since these are also statistically independent (see Appendix A). The calculation is instructive, since it shows that the first term in (8.5.2) can be identified with the decay of entropy fluctuations. It follows that the Brillouin doublet is associated with propagating pressure fluctuations at constant entropy (hence the appearance of the adiabatic speed of sound) while the Rayleigh line corresponds to non-propagating fluctuations in entropy at constant pressure.[4]

The wavelength of visible light is much greater than the nearest-neighbour spacing in liquids. Light-scattering experiments are therefore ideally suited to measurements of the Rayleigh–Brillouin spectrum at long wavelengths and provide an accurate means of measurement of properties such as the thermal diffusivity, speed of sound and sound-attenuation coefficient. However, the spectral lineshape is determined by a small number of

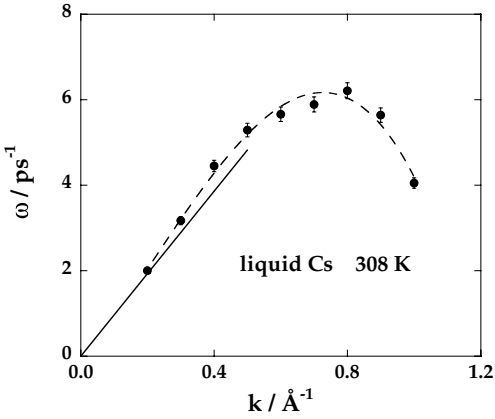

FIG. 8.3. Dispersion of the Brillouin peak in liquid caesium near the normal melting temperature. The points are the results of inelastic neutron-scattering experiments and the line shows the hydrodynamic dispersion corresponding to the experimental speed of sound, $c_S = 965\ \mathrm{m\,s^{-1}}$. After Bodensteiner *et al.*[10]

macroscopic properties that are insensitive to details either of the interactions between particles or of the molecular structure of the fluid. From the standpoint of microscopic theory the more interesting question is whether the propagating density fluctuations characteristic of the hydrodynamic regime can also be supported in simple liquids at wavelengths comparable with the spacing between particles. We have already seen in Section 7.5 that well-defined, collective excitations of the hydrodynamic type, manifesting themselves in a three-peak structure in $S(k, \omega)$, have been detected in neutron-scattering experiments on liquid caesium, but similar results have been obtained by neutron or x-ray scattering for the other alkali metals as well as for lead, mercury and aluminium.[7] Brillouin-type sidepeaks have also been seen in molecular-dynamics calculations on a variety of systems, including both the hard-sphere[8] and Lennard-Jones[9] fluids. The spectra are therefore qualitatively similar to those predicted by hydrodynamics, though there are some major differences in detail. Figure 8.3, for example, shows the dispersion of the sound-wave peak observed in neutron-scattering experiments on liquid caesium. At the smallest wavenumbers the dispersion is approximately linear, in agreement with hydrodynamics, but corresponds to a speed of propagation significantly higher than the adiabatic speed of sound. The widths of the Rayleigh and Brillouin lines are also poorly described by the hydrodynamic result. As we shall see in Section 8.6 and again in Chapter 9, a description of the density fluctuations in the range of k explored in neutron or x-ray scattering experiments requires a generalisation of the hydrodynamic approach, the effect of which is to replace the transport coefficients and thermodynamic derivatives in (8.5.4) by quantities dependent on frequency and wavenumber.

For later purposes we also require an expression for the hydrodynamic limit of the longitudinal-current autocorrelation function $C_l(k, t)$. We proceed, as before, by solving the system of equations (8.3.26) for the variable of interest, which in this case is the longitudinal particle current $\tilde{j}^z_{\mathbf{k}}(z)$. The terms in $\rho_{\mathbf{k}}$ and $T_{\mathbf{k}}$ may be omitted, since they are

uncorrelated with $\tilde{j}^z_{-\mathbf{k}}$. For z on the real axis the result is

$$\tilde{j}^z_{\mathbf{k}}(\omega) = j^z_{\mathbf{k}} \frac{-i\omega(-i\omega + ak^2)}{D_l(k,\omega)} \tag{8.5.9}$$

Thus

$$\widetilde{C}_l(k,\omega) = \frac{\omega_0^2}{-i\omega + bk^2 + c_s^2 k^2 \left(\dfrac{1}{-i\omega} + \dfrac{\gamma - 1}{-i\omega + ak^2} \right)} \tag{8.5.10}$$

The same result can be obtained from (7.4.28) and the hydrodynamic result (8.5.4).

According to (8.5.10), the spectrum of longitudinal-current fluctuations at small k behaves as

$$C_l(k,\omega) = \frac{1}{\pi} \mathrm{Re}\, \widetilde{C}_l(k,\omega) \approx \frac{\omega_0^2}{\pi\omega^2} \left(bk^2 + \frac{(\gamma - 1)ac_s^2 k^4}{\omega^2 + (ak^2)^2} \right) \tag{8.5.11}$$

Hence the longitudinal viscosity is given by a limiting operation analogous to (8.4.6) for the shear viscosity, i.e.

$$\tfrac{4}{3}\eta + \zeta = \rho m b = \pi\beta\rho m^2 \lim_{\omega\to 0} \lim_{k\to 0} \frac{\omega^2}{k^4} C_l(k,\omega) \tag{8.5.12}$$

If we now follow steps similar to those that lead to the Green–Kubo formula (8.4.10), we find that the longitudinal viscosity can be expressed in terms of the autocorrelation function of a diagonal element of the microscopic stress tensor (8.4.14):

$$\tfrac{4}{3}\eta + \zeta = \lim_{\omega\to 0} \frac{\beta}{V} \int_0^\infty \left\langle \Pi_0^{zz}(t) \Pi_0^{zz} \right\rangle \exp(i\omega t)\, \mathrm{d}t \tag{8.5.13}$$

In taking the limit $\omega = 0$ in (8.5.13) we find a discontinuity: the thermal average of Π_0^{zz} is non-zero (see (8.4.15)), so the integrand in (8.5.13) goes to a non-zero value as $t \to \infty$. The problem is overcome by subtracting the invariant part, the transport coefficient being linked only to fluctuations in the local variables. Thus

$$\tfrac{4}{3}\eta + \zeta = \frac{\beta}{V} \int_0^\infty \left\langle \left[\Pi_0^{zz}(t) - PV \right] \left[\Pi_0^{zz} - PV \right] \right\rangle \mathrm{d}t \tag{8.5.14}$$

To obtain the Green–Kubo relation for the thermal conductivity we require an expression for the rate of decay of a fluctuation in $q(\mathbf{r},t)$, the macroscopic density of heat energy; $q(\mathbf{r},t)$ is related to the entropy density by (8.3.10). We first use (8.3.11) to eliminate the local temperature from the energy equation (8.3.13). The result is

$$\left(\frac{\partial}{\partial t} - a\nabla^2 \right) \delta q(\mathbf{r},t) - \frac{\lambda T \beta_V}{\rho^2 c_V} \nabla^2 \delta\rho(\mathbf{r},t) = 0 \tag{8.5.15}$$

which, after transformation to Fourier–Laplace variables and use of (8.3.12) and the thermodynamic chain rule

$$\left(\frac{\partial S}{\partial \rho}\right)_T = -\left(\frac{\partial S}{\partial T}\right)_\rho \left(\frac{\partial T}{\partial \rho}\right)_S = -\frac{Nc_V}{T}\left(\frac{\partial T}{\partial \rho}\right)_S \tag{8.5.16}$$

gives

$$\left(-iz + ak^2\right)\tilde{q}_{\mathbf{k}}(z) + \lambda k^2 \left(\frac{\partial T}{\partial \rho}\right)_S \tilde{\rho}_{\mathbf{k}}(z) = q_{\mathbf{k}} \tag{8.5.17}$$

Next, an equation relating $\tilde{\rho}_{\mathbf{k}}(z)$ to $\widetilde{P}_{\mathbf{k}}(z)$ is obtained by taking the divergence of the Navier–Stokes equation (8.3.16) and transforming again to the variables k and z; the result in this case is

$$izm\left(-iz + bk^2\right)\tilde{\rho}_{\mathbf{k}}(z) - k^2 \widetilde{P}_{\mathbf{k}}(z) = -m\left(-iz + bk^2\right)\rho_{\mathbf{k}} \tag{8.5.18}$$

where $\mathbf{k}$ has once more been chosen perpendicular to the initial particle current. Equation (8.5.18) can now be converted into a relation for $\tilde{q}_{\mathbf{k}}(z)$ by making the substitutions

$$\widetilde{P}_{\mathbf{k}}(z) = \left(\frac{\partial P}{\partial \rho}\right)_S \tilde{\rho}_{\mathbf{k}}(z) + \frac{V}{T}\left(\frac{\partial P}{\partial S}\right)_\rho \tilde{q}_{\mathbf{k}}(z) \tag{8.5.19}$$

and

$$\rho_{\mathbf{k}} = \left(\frac{\partial \rho}{\partial P}\right)_S P_{\mathbf{k}} + \frac{V}{T}\left(\frac{\partial \rho}{\partial S}\right)_\rho q_{\mathbf{k}} \tag{8.5.20}$$

The final step is to eliminate $\tilde{\rho}_{\mathbf{k}}(z)$ between (8.5.17) and (8.5.18). The resulting expression for $\tilde{q}_{\mathbf{k}}(z)$ has some similarities with that obtained previously for $\tilde{\rho}_{\mathbf{k}}(z)$ in (8.5.1). In particular, there are two complex-conjugate poles and a single imaginary pole. At small k the local pressure and entropy are uncorrelated (see Appendix A). The problem can therefore be simplified by discarding terms proportional to $P_{\mathbf{k}}$. The lowest-order solution for $\tilde{q}_{\mathbf{k}}(z)$ then reduces to

$$\tilde{q}_{\mathbf{k}}(z) = \frac{q_{\mathbf{k}}}{-iz + D_{\mathrm{T}}k^2} \tag{8.5.21}$$

where D_{T} is the thermal diffusivity defined by (8.3.36). Equation (8.5.21) describes a purely diffusive mode, thereby confirming the fact that the Rayleigh peak in $S(k, \omega)$ is associated with the decay of non-propagating entropy fluctuations.

Our main concern is with the behaviour at small k. Since $\lim_{k\to 0} q_{\mathbf{k}} = T\Delta S$, it follows from (A.8) of Appendix A that $\langle q_{\mathbf{k}} q_{-\mathbf{k}}\rangle$ can be replaced by

$$\left\langle q_0^2 \right\rangle = T^2 N k_{\mathrm{B}} c_P \tag{8.5.22}$$

We now proceed as in the cases of the shear and longitudinal viscosities. On multiplying (8.5.21) through by $q_{-\mathbf{k}}$ and taking the thermal average, we obtain an expression for the

thermal conductivity of the form

$$\lambda = \rho c_P D_T = \frac{\beta}{VT} \lim_{\omega\to 0}\lim_{k\to 0} \frac{\omega^2}{k^2} \mathrm{Re}\langle \tilde{q}_{\mathbf{k}}(\omega) q_{-\mathbf{k}}\rangle \tag{8.5.23}$$

If we introduce a fluctuating heat current $\mathbf{J}^q_{\mathbf{k}}(t)$ defined, by virtue of (8.3.8), as the Fourier transform of

$$\mathbf{J}^q(\mathbf{r},t) = \mathbf{J}^e(\mathbf{r},t) - \frac{e+P}{\rho}\mathbf{j}(\mathbf{r},t) \tag{8.5.24}$$

we see that the energy-conservation equation (8.3.2) may be re-expressed as

$$\frac{\partial}{\partial t} q_{\mathbf{k}}(t) + i\mathbf{k}\cdot\mathbf{J}^q_{\mathbf{k}}(t) = 0 \tag{8.5.25}$$

Hence, if the z-axis is taken parallel to $\mathbf{k}$, we can rewrite (8.5.23) in typical Green–Kubo form as

$$\lambda = \frac{\beta}{VT}\int_0^\infty \langle J_0^{qz}(t) J_0^{qz}\rangle \,\mathrm{d}t \tag{8.5.26}$$

For (8.5.26) to be useful we require a microscopic expression for the heat current. Taking the Fourier transform of (8.3.2), we find that the component of the microscopic energy current in the direction of $\mathbf{k}$ is

$$-ikJ^{ez}_{\mathbf{k}} = \frac{\partial}{\partial t} e_{\mathbf{k}} = \frac{\partial}{\partial t}\sum_{i=1}^N \left(\tfrac{1}{2}m|\mathbf{u}_i|^2 + \tfrac{1}{2}\sum_{j\neq i}^N v(r_{ij})\right)\exp(-i\mathbf{k}\cdot\mathbf{r}_i) \tag{8.5.27}$$

where we have adopted the convention that the total potential energy of interaction of two particles is shared equally between them. Differentiation of the quantity inside large brackets gives rise to a term that can be treated by the methods used in calculating the microscopic stress tensor; the final result for $\mathbf{k} = 0$ is

$$J_0^{ez} = \sum_{i=1}^N u_{iz}\left(\tfrac{1}{2}m|\mathbf{u}_i|^2 + \tfrac{1}{2}\sum_{j\neq i}^N v(r_{ij})\right) - \tfrac{1}{2}\sum_{i=1}^N\sum_{j\neq i}^N \mathbf{u}_i\cdot\mathbf{r}_{ij}\frac{\partial v(r_{ij})}{\partial z_{ij}} \tag{8.5.28}$$

The current J_0^{qz} is obtained from J_0^{ez} by subtracting the term $(e+P)\sum_i u_{iz}$; with a suitable choice of frame of reference this term will be zero. Thus we can equally well write the Green–Kubo formula for λ as

$$\lambda = \frac{\beta}{VT}\int_0^\infty \langle J_0^{ez}(t) J_0^{ez}\rangle \,\mathrm{d}t \tag{8.5.29}$$

The correlation-function formulae (or the equivalent Einstein expressions) for D, η, ζ and λ have been used in simulations to determine the transport coefficients of a number of model fluids. A particularly large body of results exists for the hard-sphere fluid, some

of which have already been discussed in Section 8.4. As we saw there, the shear viscosity is in good agreement with the predictions of Enskog theory at densities up to about 80% of that corresponding to the fluid–solid transition, but close to the transition it is larger than the Enskog value by a factor of nearly two. The enhancement of the shear viscosity at high densities is linked numerically to the existence of a long-lived positive tail in the corresponding autocorrelation function. The bulk viscosity is purely potential in origin and vanishes as $\rho \to 0$, but the Enskog result for the thermal conductivity has a structure similar to that displayed for η in (8.4.21), i.e.

$$\frac{\lambda_E}{\lambda_0} = \frac{2\pi\rho d^3}{3}\left(\frac{1}{y} + 1.2 + 0.757y\right) \tag{8.5.30}$$

where $\lambda_0 = (75k_B/64d^2)(k_BT/\pi m)^{1/2}$ is the value in the low-density limit.[5] The potential term (the last term within brackets) again provides the dominant contribution at high densities, but good agreement with molecular-dynamics results is now maintained up to the freezing transition. The success of Enskog theory in the case of λ can be plausibly attributed to the absence of a significant tail in the energy-current autocorrelation function.

8.6 GENERALISED HYDRODYNAMICS

In the earlier sections of this chapter we have shown in some detail how the equations of hydrodynamics can be used to calculate the time-correlation functions of conserved variables in the long-wavelength, low-frequency limit. Two questions then arise. First, what are the scales of length and time over which it is possible to maintain the continuum description that underlies the hydrodynamic approach? Secondly, how can the hydrodynamic equations be modified to make their predictions applicable on the atomic scale, where lengths are typically of order a few ångström units and times are of order 10^{-13} s? We have seen in Chapter 7 that the behaviour of the correlation functions at short times is related to frequency sum rules involving static distribution functions descriptive of the molecular structure of the fluid. It is precisely these sum rules that are violated by hydrodynamic expressions such as (8.4.5) and (8.5.4), since the resulting frequency moments beyond zeroth order all diverge. In addition, an exponential decay, such as that in (8.4.3), cannot satisfy certain of the general properties of time-correlation functions discussed in Section 7.1. The failure of the hydrodynamic approach at short times (or high frequencies) is linked to the presence of dissipative terms in the basic hydrodynamic equations; the latter, unlike the microscopic equations of motion, are not invariant under time reversal. In this section we describe some phenomenological generalisations of the hydrodynamic equations, based on the introduction of frequency and wavenumber-dependent transport coefficients, that have been developed in attempts to bridge the gap between the hydrodynamic (small k, ω) and kinetic (large k, ω) regimes. The use of non-local transport coefficients is closely related to the memory-function approach of Section 7.3, which we develop in more systematic fashion in Chapter 9.

The ideas of *generalised hydrodynamics* are most easily illustrated by considering the example of the transverse-current correlations. Equation (8.4.3) shows that in the hydrodynamic limit the correlation function $C_t(k, t)$ decays exponentially with a relaxation time

equal to $1/\nu k^2$, where ν is the kinematic shear viscosity. The corresponding power spectrum is of lorentzian form:

$$C_t(k,\omega) = \frac{1}{\pi}\mathrm{Re}\,\widetilde{C}_t(k,\omega) = \frac{\omega_0^2}{\pi}\frac{\nu k^2}{\omega^2 + (\nu k^2)^2} \tag{8.6.1}$$

The ω^{-2} behaviour at large ω is not compatible with the exact, high-frequency sum rules such as (7.4.38), nor does (8.6.1) yield the correct free-particle limit of $C_t(k,\omega)$ at large k; that limit is gaussian in form, similar to the longitudinal free-particle limit displayed in (7.5.17). Moreover, molecular-dynamics calculations, which are the only source of "experimental" information on transverse-current fluctuations in atomic liquids, show that in an intermediate wavenumber range $C_t(k,t)$ decays in an oscillatory manner and its power spectrum has a peak at non-zero frequency, suggestive of the existence of a propagating shear mode. (Examples of the power spectra are shown later in Chapter 9, Figure 9.3.) What this means physically is that at high frequencies the fluid has insufficient time to flow in response to an applied strain rate, and instead reacts elastically in the manner of a solid. To account for the appearance of shear waves we need to extend the hydrodynamic description to include the effects of elasticity. Suppose that a shearing force is applied to a fluid. The strain at a point (x, y, z) is expressible in terms of the displacement $\mathbf{r}$ at that point and the rate of strain is expressible in terms of the velocity $\dot{\mathbf{r}}$. If the flow is purely viscous, the shearing stress (an off-diagonal component of the stress tensor $\boldsymbol{\Pi}$) is proportional to the rate-of-strain tensor and can be written as

$$\Pi^{xz} = -\eta\frac{\partial}{\partial t}\left(\frac{\partial r_x}{\partial z} + \frac{\partial r_z}{\partial x}\right) \tag{8.6.2}$$

which is the hydrodynamic form (see (8.3.15)). By contrast, if the force is applied suddenly, the instantaneous displacement is determined by the stress through a typical stress–strain relation, i.e.

$$\Pi^{xz} = -G_\infty\left(\frac{\partial r_x}{\partial z} + \frac{\partial r_z}{\partial x}\right) \tag{8.6.3}$$

where G_∞ is an instantaneous (high-frequency) modulus of rigidity. We can interpolate between these two extremes by making a *viscoelastic* approximation such that

$$\left(\frac{1}{\eta} + \frac{1}{G_\infty}\frac{\partial}{\partial t}\right)\Pi^{xz} = -\frac{\partial}{\partial t}\left(\frac{\partial r_x}{\partial z} + \frac{\partial r_z}{\partial x}\right) \tag{8.6.4}$$

By taking the Laplace transform of (8.6.4) it is easy to show that the viscoelastic approximation is equivalent to replacing η in (8.6.2) by a complex, frequency-dependent shear viscosity given by

$$\tilde{\eta}(\omega) = \frac{G_\infty}{-i\omega + 1/\tau_\mathrm{M}} \tag{8.6.5}$$

The constant $\tau_\mathrm{M} = \eta/G_\infty$ is called the Maxwell relaxation time. If $\omega\tau_\mathrm{M} \ll 1$, $\tilde{\eta}(\omega) \approx \eta$, which corresponds to purely viscous flow, but if $\omega\tau_\mathrm{M} \gg 1$, substitution of (8.6.5) in (8.6.4)

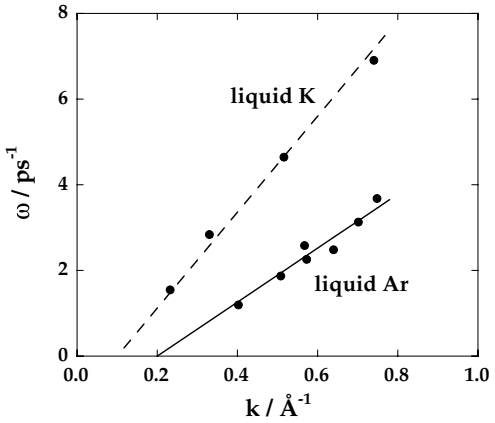

FIG. 8.4. Dispersion of the shear-wave peak derived from molecular-dynamics simulations of liquid argon[9,11] and potassium[12] for state conditions close to the triple point. The dashed line through the data for potassium is a guide to the eye; the full line for argon is drawn with a slope given by the viscoelastic expression (8.6.6) for the speed of propagation (630 m s^{-1}). Results are shown only for the range of k in which the dispersion is approximately linear.

yields a dispersion relation of the form $\omega^2 \approx (G_\infty/\rho m)k^2$, corresponding to elastic waves propagating at a speed

$$c_t = (G_\infty/\rho m)^{1/2} \tag{8.6.6}$$

Figure 8.4 shows the dispersion of the shear-wave peak observed in molecular-dynamics simulations of liquid argon and potassium at state conditions close to their respective triple points. Over the wavenumber range covered by the figure the dispersion is well described by a relation of the form $\omega = c_t(k - k_t)$, where k_t is the wavenumber below which the propagating mode vanishes. In the case of argon, for which a value of G_∞ is available from simulation, the slope of the dispersion curve is in surprisingly good agreement with that calculated from the viscoelastic approximation (8.6.6).

If account is also to be taken of non-local effects in space, the generalised shear viscosity must be a function of wavenumber as well as of frequency. The rigidity modulus is also dependent on k and related in a simple way to the second frequency moment ω_{1t}^2. These ideas can be formalised via a phenomenological generalisation of the hydrodynamic equation (8.4.2):

$$\frac{\partial}{\partial t}C_t(k,t) + k^2 \int_0^t \nu(k, t-s)C_t(k,s)\,\mathrm{d}s = 0 \tag{8.6.7}$$

The quantity $\nu(k,t)$ is a memory function; it describes a response that is non-local in both space and time and its Laplace transform $\tilde{\nu}(k,\omega)$ plays the role of a generalised kinematic viscosity. If we take the Laplace transform of (8.6.7) and compare the result with (8.4.4), we find that $\tilde{\nu}(k,\omega)$ must satisfy the constraint that

$$\lim_{\omega\to 0}\lim_{k\to 0}\tilde{\nu}(k,\omega) = \nu \tag{8.6.8}$$

where ν is the macroscopic kinematic viscosity, given by the Green–Kubo formula (8.4.10). If, on the other hand, we differentiate (8.6.7) with respect to t, set $t = 0$ and use (7.4.37), we find that

$$\nu(k, t = 0) = \frac{\omega_{1t}^2}{k^2} \equiv \frac{G_\infty(k)}{\rho m} \tag{8.6.9}$$

which acts as the definition of the k-dependent shear modulus $G_\infty(k)$. Equations (8.6.8) and (8.6.9) are useful in the construction of approximate forms of $\nu(k, t)$ that reduce to the hydrodynamic and viscoelastic expressions in the limits, respectively, $\omega \to 0$ and $\omega \to \infty$.

If molecular-dynamics results for $C_t(k, t)$ are available, values of the generalised shear viscosity $\tilde{\eta}(k, \omega) = \rho m \tilde{\nu}(k, \omega)$ can be obtained by numerical inversion of (8.6.7) while its value at infinite wavelength, $\tilde{\eta}(k = 0, \omega) \equiv \tilde{\eta}(\omega)$, is given by the Laplace transform of the stress autocorrelation function $\eta(t)$ in (8.4.10). The generalised shear viscosity is believed to be a non-analytic function of both k and ω. For example, molecular-dynamics calculations for hard spheres[13] have shown that $\eta(t)$ decays as $t^{-3/2}$ beyond about ten mean collision times, implying that $\tilde{\eta}(\omega)$ behaves as $\omega^{1/2}$ at low frequencies. If the zero-frequency shear viscosity $\eta(k) \equiv \tilde{\eta}(k, \omega = 0)$ could be expanded in a Taylor series in k about its macroscopic limit, $\eta \equiv \eta(k = 0)$, the series would start as

$$\eta(k) = \eta + \eta_2 k^2 + \cdots \tag{8.6.10}$$

since invariance under space inversion means that only even powers of k can appear. The quantity η_2 is called a Burnett coefficient. Burnett coefficients were introduced in an attempt to extend the range of validity of hydrodynamic equations through the addition of terms of higher order in the gradients of the hydrodynamic fields. However, the indications from mode-coupling theories[14] of the type to be discussed in the section that follows are that the coefficients diverge, implying that the relation between the applied gradients and the induced hydrodynamic fluxes is non-analytic in character. This conclusion is supported by the results of computer simulations of a soft-sphere (r^{-12}) fluid,[15] which are compatible with a small-k behaviour of the form

$$\eta(k) = \eta - \eta_{3/2} k^{3/2} + \cdots \tag{8.6.11}$$

where $\eta_{3/2}$ is a positive quantity. These and related calculations[16] suggest that $\eta(k)$ and other generalised transport coefficients decrease smoothly with increasing wavenumber, becoming an order of magnitude smaller than their macroscopic ($k = 0$) values when the wavelength is comparable with the interparticle spacing.

The longitudinal projections of the hydrodynamic equations can be treated in the same way through the introduction of wavenumber and frequency-dependent quantities that are generalisations of the coefficients a and b defined by (8.3.14) and (8.3.25). Similarly, the thermodynamic derivatives, which are related to static correlation functions, become functions of wavelength.[17] In particular, the macroscopic compressibility is replaced by its k-dependent generalisation, i.e. the structure factor $S(k)$ (see (3.6.11)), while the thermal pressure coefficient, which determines the coupling between momentum and energy, now contains a part that is explicitly dependent on frequency and vanishes in the limit $k \to 0$.

A scheme in which the various thermodynamic and transport coefficients are assumed to be functions only of wavenumber and not of frequency has been found to reproduce satisfactorily a large part of the molecular-dynamics results obtained for the dynamic structure factor of the hard-sphere fluid.[8] This approach breaks down, however, both for wavelengths shorter than the mean free path (corresponding to free-particle behaviour), and at densities close to crystallisation, where viscoelastic effects becomes important.

8.7 LONG-TIME TAILS IN TIME-CORRELATION FUNCTIONS

Fluctuations in the conserved hydrodynamic variables decay infinitely slowly in the long-wavelength limit. The rates of relaxation are determined by the hydrodynamic eigenvalues (8.3.31) and (8.3.35) (multiplied by $-i$), all of which vanish with k. No such property holds for the non-conserved currents that enter the Green–Kubo integrands for the transport coefficients; if it did, the transport coefficients would not be well defined. Until the late 1960s it was generally believed that away from critical points the autocorrelation functions of non-conserved variables decay exponentially at long times. This, for example, is the behaviour predicted by the Boltzmann and Enskog equations. It therefore came as a surprise when analysis of the molecular-dynamics results of Alder and Wainwright[18] on self diffusion in hard-disk ($\mathcal{D} = 2$) and hard-sphere ($\mathcal{D} = 3$) fluids showed that the velocity autocorrelation function apparently decays asymptotically as $t^{-\mathcal{D}/2}$, where $\mathcal{D}$ denotes the dimensionality of the system. Later simulations of hard-core fluids and other systems have also detected the presence of a long-time tail in the stress-tensor autocorrelation function.

The presence of a slowly decaying tail in $Z(t)$ suggests that highly collective effects make a significant contribution to the process of self diffusion. The apparent involvement of large numbers of particles makes it natural to analyse the long-time behaviour in hydrodynamic terms, and Alder and Wainwright were led in this way to a simple but convincing explanation of their results. Underlying their argument is the idea that the initial motion of a tagged particle creates around that particle a vortex or backflow, which in turn causes a retarded current to develop in the direction of the initial velocity. At low densities, where the initial direction of motion is likely to persist, the effect of the current is to reduce the drag on the particle, thereby "pushing" it onwards in the initial direction. This results in a long-lasting, positive correlation between the initial velocity and its value at later times. At high densities, on the other hand, the initial direction of motion is on average soon reversed. In this case the retarded current gives rise to an extra drag at later times and hence to an extended negative region in $Z(t)$; at very large times an enhancement of the forward motion can again be expected but the effect is likely to be undetectable. That this physical picture is basically correct was confirmed in striking fashion by observation of the velocity field that forms around a moving particle in a fluid of hard disks. A vortex pattern quickly develops; this, after a few mean collision times, matches closely the pattern obtained by numerical solution of the Navier–Stokes equation. The persistence of the tail in $Z(t)$ is therefore associated with a coupling between the motion of the tagged particle and the hydrodynamic modes of the fluid. As we shall now show, this argument can be formalised in such a way as to predict the observed $t^{-\mathcal{D}/2}$ decay at long times.[19]

Suppose that at time $t = 0$ a particle i has a component of velocity $u_{ix}(0)$ in the x-direction. After a short time, τ say, collisions will have caused the initial momentum of particle i to be shared among the ρV_τ particles in a $\mathcal{D}$-dimensional volume V_τ centred on i. Local equilibrium now exists within the volume V_τ, and particle i will be moving with a velocity $u_{ix}(\tau) \approx u_{ix}(0)/\rho V_\tau$. (We have assumed, for simplicity, that the neighbours of i are initially at rest.) Further decay in the velocity $u_{ix}(t)$ for $t > \tau$ will occur as the result of enlargement of the volume V_τ, i.e. from the spread of the velocity field around particle i. At large times the dominant contribution to the growth of V_τ will come from diffusion of the transverse component of the velocity field and the radius of V_τ will therefore increase as $(\nu t)^{1/2}$. Thus $V_\tau \sim (\nu t)^{3/2}$ in the three-dimensional case, from which it follows that $Z(t) \sim (\nu t)^{-3/2}$. This argument assumes that particle i remains at the centre of V_τ; if the diffusive motion of i is taken into account it can be shown that

$$Z(t) \sim \left[(D + \nu)t\right]^{-3/2} \tag{8.7.1}$$

The analogous result in two dimensions implies that a self-diffusion coefficient does not exist, because the integral of $Z(t)$ diverges logarithmically.

The form of (8.7.1) has been confirmed by a number of more sophisticated calculations. In the case of hard-core fluids these include a microscopic treatment based on kinetic theory in which account is taken of the effect of correlated collision sequences (the ring collisions of Section 7.2) along with that of uncorrelated, binary collisions.[20] Though limited to low densities, the calculation shows that the velocity, stress-tensor and energy-current autocorrelation functions all decay as $t^{-\mathcal{D}/2}$; it also yields explicit expressions for the coefficients of the long-time tails. A more phenomenological approach has also been developed in which the existence of the long-time tails is explained by simple arguments concerning the decay of fluctuations into pairs of hydrodynamic modes. Since the physical content of this work is closely related to the mode-coupling formalism to be discussed in Chapter 9, we give here a brief derivation of the result obtained in three dimensions for the velocity autocorrelation function.[21]

The definition (7.1.3) of a time-correlation function involves an equilibrium ensemble average over the initial phase-space coordinates of the system. This average can be replaced by a constrained ensemble average, characterised by an initial position $\mathbf{r}_0$ and initial velocity $\mathbf{u}_0$ of a tagged particle i, which is then integrated over all $\mathbf{r}_0$ and $\mathbf{u}_0$. The definition of $Z(t)$ is thereby reformulated as

$$\begin{aligned} Z(t) &= \langle u_{ix}(t)u_{ix}\rangle \\ &= \int \mathrm{d}\mathbf{r}_0 \int \mathrm{d}\mathbf{u}_0\, u_{0x}\langle u_{ix}(t)\delta(\mathbf{u}_i - \mathbf{u}_0)\delta(\mathbf{r}_i - \mathbf{r}_0)\rangle \end{aligned} \tag{8.7.2}$$

The constrained average in (8.7.2) can be written as a non-equilibrium ensemble average (subscript n.e.), defined through the relation

$$\langle u_{ix}(t)\delta(\mathbf{u}_i - \mathbf{u}_0)\delta(\mathbf{r}_i - \mathbf{r}_0)\rangle = \langle u_{ix}(t)\rangle_{\text{n.e.}}\langle\delta(\mathbf{u}_i - \mathbf{u}_0)\delta(\mathbf{r}_i - \mathbf{r}_0)\rangle \tag{8.7.3}$$

In the canonical ensemble the equilibrium average on the right-hand side of (8.7.3) is equal to $1/N$ times the single-particle distribution function defined by (2.1.15) (taken for $n = 1$)

but with $\mathbf{p}$ replaced by $\mathbf{u}$ as independent variable. Equations (8.7.2) and (8.7.3) can therefore be combined to give

$$Z(t) = \frac{1}{V}\int \mathrm{d}\mathbf{r}_0 \int \mathrm{d}\mathbf{u}_0\, \phi_{\mathrm{M}}(\mathbf{u}_0) u_{0x} \langle u_{ix}(t)\rangle_{\mathrm{n.e.}} \tag{8.7.4}$$

where $\phi_{\mathrm{M}}(\mathbf{u}_0)$ is the Maxwell distribution (2.1.28). By defining a tagged-particle distribution function in the non-equilibrium ensemble as

$$f^{(s)}(\mathbf{r}, \mathbf{u}; t) = \langle \delta[\mathbf{r}_i(t) - \mathbf{r}]\delta[\mathbf{u}_i(t) - \mathbf{u}]\rangle_{\mathrm{n.e.}} \tag{8.7.5}$$

we can rewrite the non-equilibrium average in (8.7.4) as

$$\langle u_{ix}(t)\rangle_{\mathrm{n.e.}} = \int \mathrm{d}\mathbf{r} \int \mathrm{d}\mathbf{u}\, u_x f^{(s)}(\mathbf{r}, \mathbf{u}; t) \tag{8.7.6}$$

The calculation thus far is exact. To make progress we assume that $f^{(s)}(\mathbf{r}, \mathbf{u}; t)$ relaxes towards the corresponding local-equilibrium form on a timescale that is fast in comparison with the rate of decay of $Z(t)$. The long-time behaviour of the non-equilibrium average (8.7.6) is then obtained by replacing $f^{(s)}(\mathbf{r}, \mathbf{u}; t)$ by the tagged-particle analogue of (8.1.5) to give

$$\langle u_{ix}(t)\rangle_{\mathrm{n.e.}} = \int \rho^{(s)}(\mathbf{r}, t) u_x(\mathbf{r}, t)\, \mathrm{d}\mathbf{r} \tag{8.7.7}$$

If this result is in turn substituted in (8.7.4), and the hydrodynamic variables $\mathbf{u}(\mathbf{r}, t)$ and $\rho^{(s)}(\mathbf{r}, t)$ are replaced by the sums of their Fourier components, we find that

$$\begin{aligned} Z(t) = \frac{1}{3V}\int \mathrm{d}\mathbf{r}_0 \int \mathrm{d}\mathbf{u}_0\, \phi_{\mathrm{M}}(\mathbf{u}_0) \\ \times \frac{1}{V^2}\sum_{\mathbf{k}}\sum_{\mathbf{k}'} \rho^{(s)}_{\mathbf{k}'}(t)\mathbf{u}_{\mathbf{k}}(t)\cdot\mathbf{u}_0 \int \exp[-i(\mathbf{k}+\mathbf{k}')\cdot\mathbf{r}]\,\mathrm{d}\mathbf{r} \end{aligned} \tag{8.7.8}$$

The integral over $\mathbf{r}$ is equal to $V\delta_{\mathbf{k},-\mathbf{k}'}$ and (8.7.8) therefore reduces to

$$Z(t) = \frac{1}{3V}\int \mathrm{d}\mathbf{r}_0 \int \mathrm{d}\mathbf{u}_0\, \phi_{\mathrm{M}}(\mathbf{u}_0) \frac{1}{V}\sum_{\mathbf{k}} \rho^{(s)}_{-\mathbf{k}}(t)\mathbf{u}_{\mathbf{k}}(t)\cdot\mathbf{u}_0 \tag{8.7.9}$$

Equation (8.7.9) is said to be of "mode-coupling" form, because $Z(t)$ is expressed as a sum of products of pairs of hydrodynamic variables. We assume, in addition, that at times much longer than the mean collision time the decay of $Z(t)$ is dominated by the long-wavelength components of the hydrodynamic fields and that the time evolution of the latter is described by the equations of linearised hydrodynamics. The quantity $\rho^{(s)}_{-\mathbf{k}}(t)$ is then given by (8.2.5), while the hydrodynamic velocity field is conveniently divided into its longitudinal and transverse parts:

$$\mathbf{u}_{\mathbf{k}}(t) = \mathbf{u}_{\mathbf{k}l}(t) + \mathbf{u}_{\mathbf{k}t}(t) \tag{8.7.10}$$

The term $\mathbf{u}_{\mathbf{k}t}(t)$ satisfies the transverse-current diffusion equation (8.4.1) (with $\mathbf{j}_{\mathbf{k}t} = \rho\mathbf{u}_{\mathbf{k}t}$), the solution to which is

$$\mathbf{u}_{\mathbf{k}t}(t) = \mathbf{u}_{\mathbf{k}t}\exp\bigl(-\nu k^2 t\bigr) \tag{8.7.11}$$

The longitudinal velocity field may be treated in a similar way, but its contribution to $Z(t)$ turns out to decay exponentially, the physical reason for this being the fact that the momentum of the tagged particle is carried away by the propagating sound waves. Hence the long-time behaviour of $Z(t)$ is entirely determined by the transverse velocity field. Finally, the choice of initial conditions implies that

$$\rho_{-\mathbf{k}}^{(s)} = \exp(i\mathbf{k}\cdot\mathbf{r}_0) \tag{8.7.12a}$$

$$\mathbf{j}_{\mathbf{k}} = \rho\mathbf{u}_{\mathbf{k}} = \mathbf{u}_0\exp(-i\mathbf{k}\cdot\mathbf{r}_0) \tag{8.7.12b}$$

An expression for $Z(t)$ is now obtained by substituting (8.7.11), (8.7.12a) and the transverse projection of (8.7.12b) into (8.7.9) (remembering that there are two transverse components), and integrating over $\mathbf{r}_0$ and $\mathbf{u}_0$. The result is

$$Z(t) = \frac{2k_{\mathrm{B}}T}{3\rho m V}\sum_{\mathbf{k}}\exp\bigl[-(D+\nu)k^2 t\bigr] \tag{8.7.13}$$

or, in the thermodynamic limit:

$$Z(t) = \frac{2k_{\mathrm{B}}T}{3\rho m}(2\pi)^{-3}\int\exp\bigl[-(D+\nu)k^2 t\bigr]\,\mathrm{d}\mathbf{k} \tag{8.7.14}$$

Integration over all wavevectors is a questionable procedure, since the hydrodynamic equations on which (8.7.14) is based are not valid when k is large. However, we are interested only in the asymptotic form of $Z(t)$, and the main contribution to the integral comes from wavenumbers such that $k \approx [(D+\nu)t]^{-1/2}$; this is in the hydrodynamic range whenever t is much larger than typical microscopic times ($\sim 10^{-13}$) s. Alternatively, a natural upper limit on k can be introduced by a more careful choice of the initial spatial distribution of tagged particles. Use of such a cut-off has no effect on the predicted long-time behaviour that results from carrying out the integration in (8.7.14), namely

$$Z(t) \sim \frac{2k_{\mathrm{B}}T}{3\rho m}\bigl[4\pi(D+\nu)t\bigr]^{-3/2}, \quad t\to\infty \tag{8.7.15}$$

This has the same general form as (8.7.1) but it also provides an explicit expression for the coefficient of the long-time tail.

The result in (8.7.15) has been confirmed by molecular-dynamics calculations for systems of hard discs and of particles interacting through a Lennard-Jones potential truncated at $r = 2^{1/6}\sigma$, the separation at which $v(r)$ has its minimum value; the simulations are difficult to carry out with the necessary precision because the long-time tail is very weak.[22] Results obtained for the truncated Lennard-Jones potential are shown in Figure 8.5, where

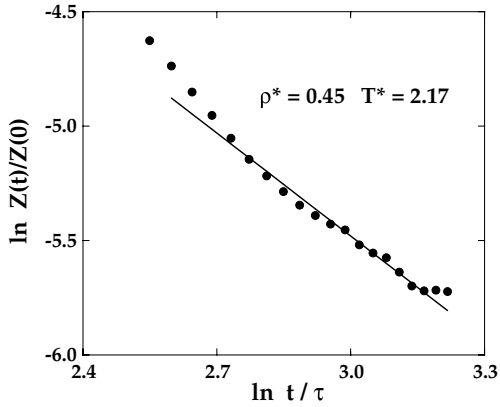

FIG. 8.5. Log–log plot of the velocity autocorrelation function versus time for a system of particles interacting through a truncated Lennard-Jones potential. The points are molecular-dynamics results and the line is drawn with a slope equal to $-\frac{3}{2}$. The unit of time is $\tau = (m\sigma^2/48\varepsilon)^{1/2}$. After Levesque and Ashurst.[22]

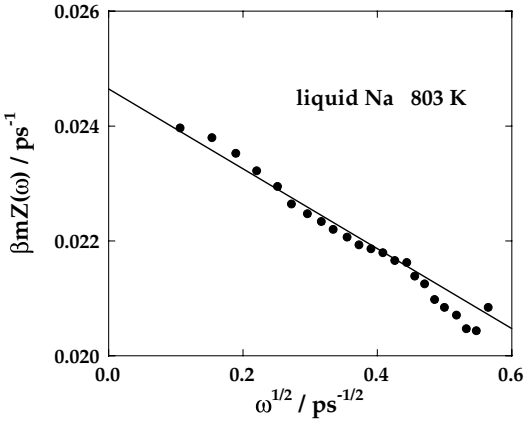

FIG. 8.6. Power spectrum of the velocity autocorrelation function of liquid sodium as a function of $\omega^{1/2}$. The points are derived from inelastic neutron-scattering measurements and the line is a least-squares fit to the data. After Morkel *et al*.[23]

$Z(t)$ is plotted versus t on a log–log scale. If (5.3.5) is used to define an effective hard-sphere diameter for the particles, the onset of the asymptotic behaviour is found to come after approximately 18 mean collision times. The predicted long-time behaviour of $Z(t)$ implies that at low frequencies its Fourier transform behaves as

$$Z(\omega) = \frac{D}{\pi}\left[1 - (\omega_0/\omega)^{1/2} + \cdots\right] \tag{8.7.16}$$

where ω_0 is related to the transport coefficients D and ν. Experimentally, evidence for the presence of a long-time tail can be derived from neutron-scattering measurements of the

self dynamic structure factor, provided results are obtained at sufficiently small values of k to allow the extrapolation required in (8.2.18) to be successfully carried through. Figure 8.6 shows some results obtained for liquid sodium at a temperature well above the melting point (the effect at low temperatures is too weak to be detectable). Not only is the square-root dependence on ω well reproduced, but the value obtained for ω_0 from a least-squares fit to the data lies within 2% of that predicted by mode-coupling theory.

8.8 DYNAMICS OF SUPERCOOLED LIQUIDS

When a liquid is slowly cooled (or compressed) it normally undergoes a transition to an ordered, crystalline phase at a temperature located on the equilibrium liquid–solid coexistence curve. However, if the rate of cooling (or compression) is sufficiently rapid, crystallisation can be by-passed; in that case the liquid is gradually transformed into an amorphous solid or glass. The glass-transition temperature T_G is less than the freezing temperature, but its value depends on factors such as the cooling rate and the diagnostic used to locate the transition; it is not an intrinsic property of the system. Relaxation times in the supercooled liquid measured, for example, in dielectric or shear-stress relaxation experiments, increase dramatically with decreasing temperature and close to the glass transition become comparable with macroscopic time-scales. A rough but useful estimate of T_G is provided by the viscoelastic theory of Section 8.6, which shows that a crossover from viscous to elastic behaviour can be expected when the structural relaxation time of the system becomes of the order of the Maxwell relaxation time, defined as the ratio of shear viscosity to shear modulus, $\tau_M = \eta/G_\infty$. The shear modulus is of order 10^{10} erg cm^{-1} for most materials and is only weakly dependent on temperature, but the shear viscosity rises by many orders of magnitude as the temperature approaches T_G. An implicit definition of T_G is obtained by identifying τ_M with some experimental time-scale, τ_{exp}. A choice of 10^3 s for τ_{exp} leads to the conventional definition of T_G as the temperature at which the viscosity reaches a value of 10^{13} poise (1 P $\equiv$ 0.1 N s m^{-2}). Below this temperature, the system exists in a metastable state having a disordered, liquid-like structure but with mechanical properties similar to those of a crystalline solid. The freezing-out of the translational and rotational degrees of freedom at the glass transition leads in many cases to anomalies in the temperature dependence of thermodynamic properties such as the specific heat. The change in behaviour at T_G is therefore described as a "thermodynamic" or "calorimetric" phase transition, though its nature is very different from that of an equilibrium phase transition.

Glass-forming liquids appear to fall into one of two broad classes: "strong" and "fragile".[24] The difference between the two is particularly evident in the way in which the viscosity changes with temperature, as exemplified by the Arrhenius plots shown in Figure 8.7. Strong glass formers are covalently bonded, network-forming substances such as silica; the network already exists in the high-temperature melt and gradually strengthens as the liquid is supercooled. The calorimetric anomalies near T_G are weak, or may be absent altogether, and the Arrhenius plots are essentially linear, implying that transport in the liquid is largely governed by thermally activated processes or "barrier hopping". The anomalies are stronger for the ionic and organic liquids that make up the class of fragile glass formers. The Arrhenius plots of such materials show a marked change in curvature

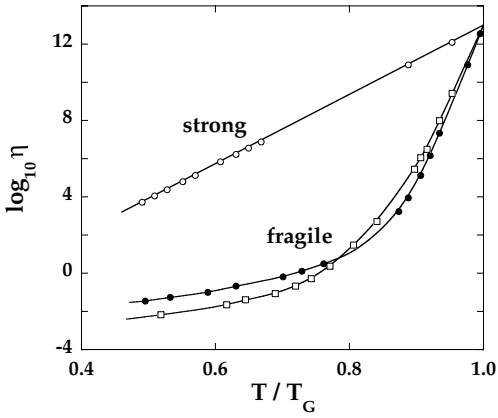

FIG. 8.7. Arrhenius plots of the shear viscosities (in poise) of three glass-forming liquids, showing the difference in behaviour between strong and fragile glass formers. Open circles: silica; squares: o-terphenyl; filled circles: an ionic melt of composition $[KNO_3]_{0.6}[Ca(NO)_3)_2]_{0.4}$. After Angell.[24]

at a temperature T_C lying some 10 to 20% above T_G; this is suggestive of a qualitative change in character of the microscopic dynamics over a narrow temperature interval. When $T \approx T_C$, the Maxwell relaxation time is in the nanosecond range. This is a time-scale well suited to studies of the dynamics by neutron and light-scattering experiments and other experimental probes as well as by molecular-dynamics simulation, and there is now ample evidence to show that as the temperature is lowered towards T_C there is a dramatic slowing down in the decay of time-dependent correlation functions. The crossover in behaviour near T_C seen, for example, in Figure 8.7, corresponds to what is called a *kinetic glass transition*. Experiment and simulation also show that structural and thermodynamic properties vary smoothly with temperature in the region of the transition. It is therefore reasonable to suppose that the supercooled liquid remains in a state of thermodynamic equilibrium and that equilibrium statistical mechanics applies once crystallisation has been by-passed. This is the key assumption underlying the mode-coupling theory of the transition, which we describe later in Section 9.6.

The nature of the changes that take place at the kinetic glass transition are well illustrated by the results shown in Figures 8.8 and 8.9. Those in Figure 8.8 are taken from a simulation of a binary,[26] soft-sphere (r^{-12}) fluid and show the behaviour for one of the two species of the probability density

$$W(r,t) = 4\pi r^2 G_s(r,t) \tag{8.8.1}$$

where $G_s(r,t)$ is the self part (7.4.19a) of the van Hove function; the quantity $W(r,t)\,\mathrm{d}r$ is the probability of finding a particle at time t at a distance r from its position at $t = 0$. The thermodynamic state of the system is specified by a single coupling constant, Γ, defined in a manner similar to (5.3.13) but generalised to allow for the two-component nature of the system. A decrease in temperature is therefore strictly equivalent to an increase in density. The inset to the figure shows the results obtained for three different times at a value of Γ corresponding to a temperature above T_C. The curve has a single peak, which moves

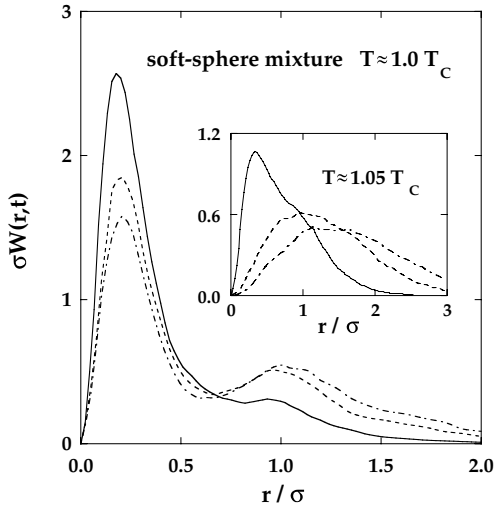

FIG. 8.8. Molecular-dynamics results for the probability density for diffusion of particles of one species in a two-component soft-sphere fluid at temperatures in the supercooled region. See text for details. Results are shown for three different values of the reduced time $t^* = t/\tau$. Full curves: $t^* = 100$; dashes: $t^* = 300$; chain curves: $t^* = 500$. For argon-like values of the potential parameters and particle masses, $\tau \approx 2$ ps; σ is an averaged size parameter. After Barrat *et al.*[25]

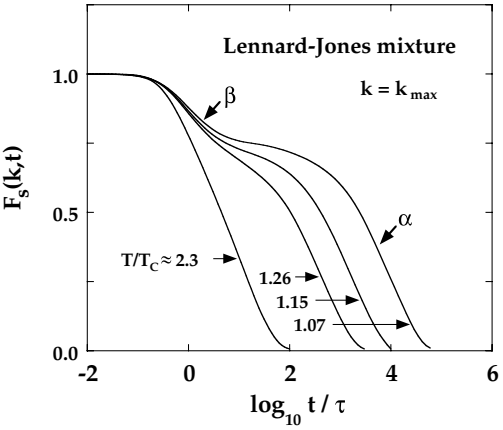

FIG. 8.9. Molecular-dynamics results for the self intermediate scattering function for particles of one species in a two-component Lennard-Jones fluid at temperatures in the supercooled region; $k_{\max}$ is the wavenumber corresponding to the main peak in the static structure factor. The labels α, β mark the two different relaxation regimes discussed in the text. For argon-like values of the potential parameters and particle masses, the unit of time is $\tau \approx 0.3$ ps. After Kob and Andersen.[27]

to larger r according to a $t^{1/2}$ law, in agreement with the result derived from Fick's law (see (8.2.8)). However, the qualitative behaviour changes dramatically above a threshold value of Γ, which can be identified with the crossover value Γ_{C}. The peak in $W(r,t)$ now

appears to be frozen at a fixed value of r and its amplitude decreases only slowly with time as a secondary maximum builds up at a distance from the main peak roughly equal to the mean spacing between particles. The physical interpretation of this bimodal distribution is clear: most atoms vibrate around fixed, disordered positions, but some diffuse slowly by correlated hopping to neighbouring sites. The two values of Γ for which the results are shown correspond to temperatures differing by less than 6%. Thus the diffusion mechanism changes very rapidly from one that is hydrodynamic-like to one consisting of a succession of activated jumps.

The same, pronounced slowing down of the single-particle motion as a threshold temperature is reached is also visible in the behaviour of the self intermediate scattering function $F_s(k,t)$. Some results obtained by molecular-dynamics calculations for a binary Lennard-Jones system are shown in Figure 8.9, where time is plotted on a logarithmic scale. At high temperatures, $F_s(k,t)$ relaxes to zero in nearly exponential fashion. However, as the temperature is lowered into the supercooled region, the decay becomes very much slower and its exponential character is lost. As T approaches T_C, the relaxation proceeds in two, increasingly well-separated steps. After a fast initial decay on the time-scale of an inverse Einstein frequency, a first step (β-relaxation) leads to a plateau, where the function remains almost constant over two or more decades in time. The plateau is followed by a second step (α-relaxation) in which the correlation function finally decays to zero. The width of the plateau increases rapidly as the temperature is reduced. Eventually, when the temperature is sufficiently low, α-relaxation can be expected to set in only at times longer than those accessible in a simulation. The correlation function will then appear to level off at a non-zero value, signalling the onset of non-ergodic behaviour, at least on the (nanosecond) time-scale of the simulation. The plateau value varies with k, but the general pattern seen in Figure 8.9 remains much the same over a wide range of molecular-scale wavenumber.

The decay of collective density fluctuations, as described by the full intermediate scattering function $F(k,t)$ defined by (7.4.20) and measurable either experimentally or by simulation, shows a qualitatively similar behaviour to that of the single-particle function. The plateau value of $F(k,t)$ is analogous to the Debye–Waller factor of a solid; it provides a measure of the "structural arrest" in the fluid, which persists for times that increase rapidly with decreasing temperature. Over a temperature range just above T_C, the decay of either function in the α-relaxation regime, normalised by its value at $t = 0$, can be accurately represented by a function of the form

$$f(t) = f_k \Phi(t^*) \tag{8.8.2}$$

where f_k is the plateau value, $t^* \equiv t/\tau_k(T)$ and $\Phi(t^*)$ is a universal scaling function. The wavenumber and temperature dependence of the decay enter only through the relaxation time $\tau_k(T)$ and the correlation functions are said to satisfy a "time–temperature superposition" principle. The scaling function is distinctly non-exponential, but is generally well-approximated by a Kohlrausch stretched-exponential function, i.e.

$$\Phi(t^*) \approx \exp\left[-(t^*)^\beta\right] \tag{8.8.3}$$

where the exponent β (< 1 for "stretching") is material and wavenumber dependent but independent of temperature.[28] Stretched-exponential behaviour is typical of relaxation

processes in which the observed rate is determined by a wide distribution of relaxation times.

NOTES AND REFERENCES

1. Rahman, A., *Phys. Rev.* **136**, A405 (1964). Deviations from gaussian behaviour increase rapidly as a liquid is supercooled: see, e.g., Bernu, B., Hansen, J.P., Hiwatari, Y. and Pastore, G., *Phys. Rev. A* **36**, 4891 (1987).
2. Landau, L.D. and Lifshitz, E.M., "Fluid Mechanics", 2nd edn. Butterworth-Heinemann, Oxford, 1987, p. 44.
3. See, e.g., Reif, F., "Fundamentals of Statistical and Thermal Physics". McGraw-Hill, New York, 1965, p. 168.
4. (a) Mountain, R.D., *Rev. Mod. Phys.* **38**, 205 (1966). (b) Berne, B.J. and Pecora, R., "Dynamic Light Scattering". John Wiley, New York, 1976.
5. Chapman, S. and Cowling, T.G., "The Mathematical Theory of Non-Uniform Gases", 3rd edn. Cambridge University Press, Cambridge, 1970, p. 308. For a simplified discussion of the Boltzmann and Enskog equations see, e.g., Reed, T.M. and Gubbins, K.E., "Applied Statistical Mechanics". McGraw-Hill, New York, 1973.
6. This is not the same effect as the $t^{-3/2}$ tail referred to in Sections 8.6 and 8.8.
7. A particularly comprehensive neutron-scattering study is that of liquid Rb by Copley, J.R.D. and Rowe, J.M., *Phys. Rev. A* **9**, 1656 (1974). For inelastic x-ray scattering and references to earlier scattering experiments on liquid metals see, e.g., Scopigno, T., Balucani, U., Ruocco, G. and Sette, F., *Phys. Rev. E* **65**, 031205 (2002).
8. Alley, W.E., Alder, B.J. and Yip, S., *Phys. Rev. A* **27**, 3174 (1983).
9. Levesque, D., Verlet, L. and Kürkijarvi, J., *Phys. Rev. A* **7**, 1690 (1973).
10. Bodensteiner, T., Morkel, C., Gläser, W. and Dorner, B., *Phys. Rev. A* **45**, 5709 (1992); erratum: *Phys. Rev. A* **46**, 3574 (1992).
11. Rahman, A., *In* "Neutron Inelastic Scattering", vol. 1. IAEA, Vienna, 1968.
12. Jacucci, G. and McDonald, I.R., *Mol. Phys.* **39**, 515 (1980).
13. Erpenbeck, J.J. and Wood, W.W., *J. Stat. Phys.* **24**, 455 (1981).
14. Keyes, T. and Oppenheim, I., *Physica* **70**, 100 (1973).
15. Evans, D.J., *Mol. Phys.* **47**, 1165 (1982).
16. (a) Alley, W.E. and Alder, B.J., *Phys. Rev. A* **27**, 3158 (1983). (b) Kambayashi, S. and Kahl, G., *Phys. Rev. A* **46**, 3255 (1992).
17. Schofield, P., *Proc. Phys. Soc.* **88**, 149 (1966).
18. Alder, B.J. and Wainwright, T.E., *Phys. Rev. Lett.* **18**, 988 (1967). (b) Alder, B.J. and Wainwright, T.E., *Phys. Rev. A* **1**, 18 (1970).
19. Pomeau, Y. and Résibois, P., *Phys. Rep.* **19**, 63 (1975).
20. (a) Dorfman, J.R. and Cohen, E.G.D., *Phys. Rev. A* **6**, 776 (1972). (b) Dorfman, J.R. and Cohen, E.G.D., *Phys. Rev. A* **12**, 292 (1975).
21. (a) Ernst, M.H., Hauge, E.H. and van Leeuwen, J.M.J., *Phys. Rev. A* **4**, 2055 (1971). (b) Erpenbeck, J.J. and Wood, W.W., *Phys. Rev. A* **26**, 1648 (1982).
22. Levesque, D. and Ashurst, W.T., *Phys. Rev. Lett.* **33**, 277 (1974). The conclusions of this paper were later confirmed, with much higher precision, by simulations of a lattice-gas model for which the equations of motion can be solved exactly: see van der Hoef, M.A. and Frenkel, D., *Phys. Rev. A* **41**, 4277 (1990).
23. Morkel, C., Gronemeyer, C., Gläser, W. and Bosse, J., *Phys. Rev. Lett.* **58**, 1873 (1987).
24. This classification is due to Angell, C.A., *J. Phys. Chem. Solids* **49**, 863 (1988).
25. Barrat, J.L., Roux, J.N. and Hansen, J.P., *Chem. Phys.* **149**, 198 (1990).
26. Simulations of the glass transition are commonly carried out on mixed systems as a device to inhibit crystallisation.
27. Kob, W. and Andersen, H.C., *Phys. Rev. E* **52**, 4134 (1995).
28. The conventional use of β for the Kohlrausch exponent is unfortunate, since it refers to the decay in the α-relaxation regime.